

**TECTONIC EVOLUTION OF THE CONTAYA ARCH  
UCAYALI BASIN, PERU**

A Thesis

by

LUIS D. NAVARRO ZELASCO

Submitted to the Office of Graduate Studies of  
Texas A&M University  
in partial fulfillment of the requirements for the degree of

MASTER OF SCIENCE

May 2010

Major Subject: Geology

**TECTONIC EVOLUTION OF THE CONTAYA ARCH  
UCAYALI BASIN, PERU**

A Thesis

by

**LUIS D. NAVARRO ZELASCO**

Submitted to the Office of Graduate Studies of  
Texas A&M University  
in partial fulfillment of the requirements for the degree of

**MASTER OF SCIENCE**

Approved by:

Chair of Committee,	John R. Hopper
Committee Members,	David Wiltschko
	Walter Ayers
Head of Department,	Andreas Kronenberg

May 2010

Major Subject: Geology

**ABSTRACT**

Tectonic Evolution of the Contaya Arch, Ucayali Basin, Peru.

(May 2010)

Luis D. Navarro Zelasco, B.En., Universidad San Agustín

Chair of Advisory Committee: Dr. John R. Hopper

The Contaya arch is an elongated topographic high that divides the Huallaga, Marañón and Ucayali basins in the Peruvian Amazonian plain. Its position well into the foreland basin and well inland from the main Andean thrust belt has proven to be enigmatic. Although it is often considered to be a single structural feature with a single origin, we show here that the Contaya arch is composed of distinct structures with different structural styles and different geologic histories: The main structures include the Contamana high, Contaya high, and Moa divisor. The Contamana high is limited by high angle reverse faults with a NW-SE orientation parallel to the Andean fold and thrust belt. This structure formed in the Tertiary, most probably in the Miocene after deposition of the Pozo Formation sands and shales. To the east of this is the Contaya high. This structure originally formed during the Triassic-Jurassic and was later reactivated in the Tertiary. The easternmost structure, the Moa divisor, separates the Ucayali basin from the Acre basin in Brazil. It is bounded by a high-angle, thick-skinned reverse fault. It appears to be a reactivated normal fault that formed in the Paleozoic during rifting and deposition of the Mitu Formation. From 10 to 4 Ma the subducted Nazca ridge was

located beneath the Peruvian fold and thrust belt in the area where the Contamana high, Contaya high and Moa divisor are located. We suggest that the uplift of the Moa Divisor and the Contamana high as NW-SE oriented structures bounded by high-angle, thick-skinned reverse faults and the reactivation of the Contaya high during the Miocene is related to the subduction of the Nazca ridge from 10 Ma to present.

## TABLE OF CONTENTS

	Page
ABSTRACT .....	iii
TABLE OF CONTENTS .....	v
LIST OF FIGURES.....	vi
LIST OF TABLES .....	viii
 CHAPTER	
I INTRODUCTION.....	1
II BACKGROUND AND TECTONIC SETTING.....	5
Tectonic and geodynamic evolution of western South America....	5
Stratigraphic evolution of the Marañon and Ucayali basins .....	8
Subduction of the Nazca ridge and Inca plateau .....	15
III DATA AND METHODS.....	19
IV RESULTS AND DISCUSSION .....	26
Discussion .....	37
V CONCLUSIONS .....	44
REFERENCES .....	45
VITA .....	49

## LIST OF FIGURES

FIGURE	Page
1	Comparison of steep subduction and flat slab subduction and their effects on the deformation in the overriding plate..... 2
2	Location map showing the positive structures that divide the Marañón, Huallaga and Ucayali basins ..... 4
3	Tectonostratigraphic evolution of the Western border of South America between 5 and 9 South..... 7
4	Stratigraphic column for the Huallaga, Marañón and Ucayali basins..... 10
5	Reconstruction of the subduction history of Nazca ridge and Inca plateau 18
6	Grayscale satellite image showing the interpreted 2D seismic lines and wells used in this study..... 21
7	Regional well correlation..... 22
8	Seismic sections location map..... 27
9	Seismic section BB' ..... 29
10	Seismic section CC' ..... 30
11	Seismic section EE' ..... 32
12	Seismic section DD' ..... 33
13	Seismic section AA' ..... 35
14	Seismic section AA' flattened at the base Cretaceous unconformity horizon..... 36
15	Time structure map at Chonta limestone horizon ..... 38

FIGURE	Page
16 Reconstruction of the subduction history of the Nazca ridge and Inca plateau at 16 Ma and 10 Ma .....	42
17 Present day location of the Nazca ridge and Inca plateau and seismological cross section. ....	43

**LIST OF TABLES**

TABLE		Page
1	Wells used in this study.....	19



## CHAPTER I

### INTRODUCTION

Andean-type subduction occurs when an oceanic plate converges and descends beneath a convergent continental plate. Along the western edge of South America, the Nazca plate is subducting beneath the South American plate, causing compression and uplift of the Andes mountain chain.

Along strike, the Andean margin is marked by alternating segments of flat slab subduction and steep subduction, producing complex and highly variable deformation in the upper plate (Gutscher, 2002). In the Peruvian segment much of this variability is a result of the subducting Nazca ridge and the Inca oceanic plateau between 5° and 9° S. Gutscher et al. (2000) showed that the subduction of buoyant, thickened oceanic crust can produce segments of flat slab subduction along the Andes. He observed that in these segments, higher interplate coupling enables stress and deformation to be transmitted as much as 250-800 km from the trench in the overriding upper plate (fig. 1). In addition, because these features on the downgoing plate are oblique with respect to the convergence direction, their effects on subduction should migrate along the plate boundary. Rosenbaum et al. (2005) showed that the spatial and temporal distribution of ore deposits in the Peruvian Andes correlates strongly with the subduction of the Nazca ridge and Inca plateau in just this manner.

---

This thesis follows the style of Tectonophysics.

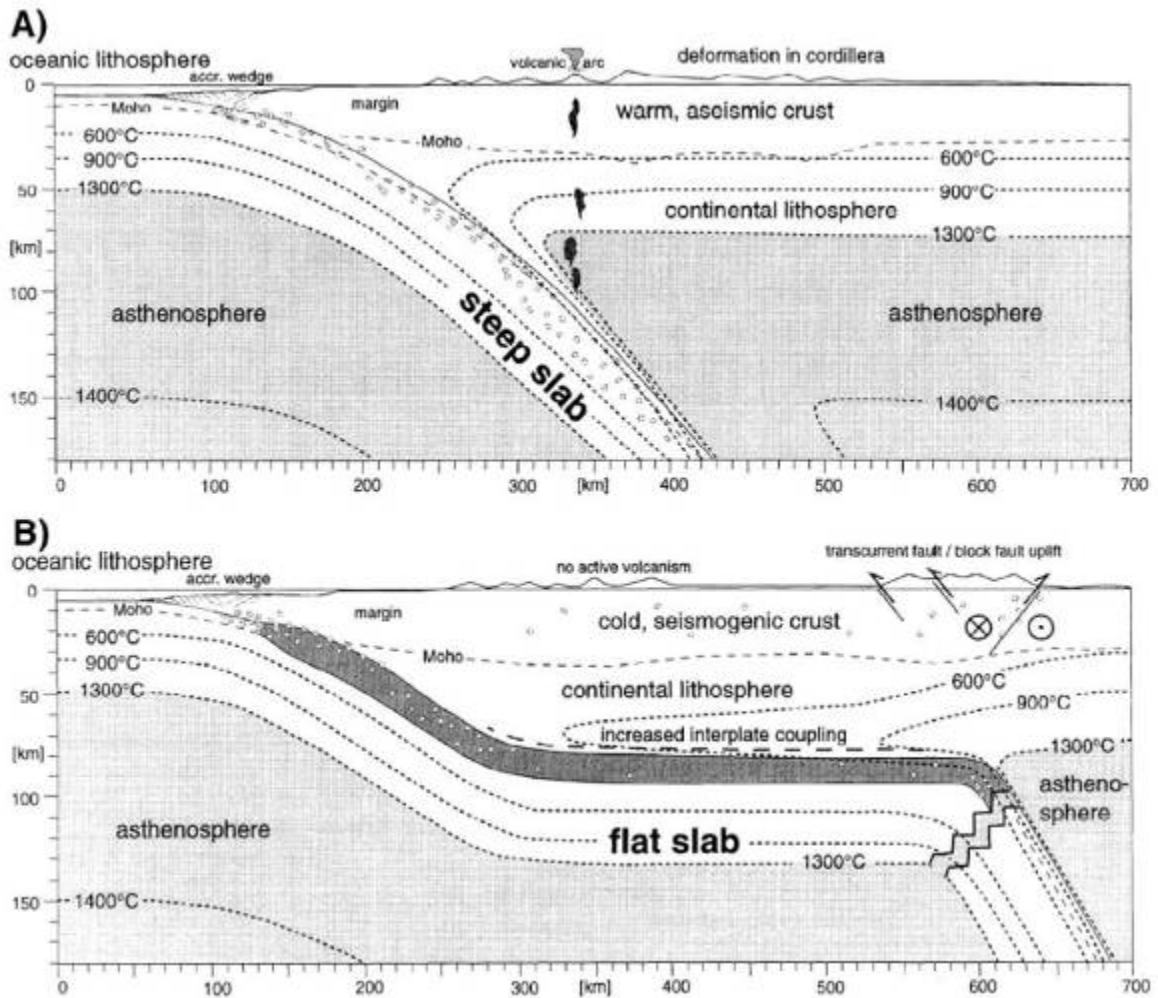


Figure 1. Comparison of steep subduction (a) and flat slab subduction (b) and their effects on the deformation in the overriding plate. From Gutscher 2002.

An unresolved issue from previous work in the Peruvian basins east of the main Andean thrust belt is to establish the extent to which deformation in the overriding plate originates as a result of subduction of anomalous features along the downgoing plate. In this contribution, we examine a number of uplifted structures in the southern Marañón, Huallaga and Ucayali basins in the central part of the Peruvian Amazonian rain forest

between 5° and 9° S to determine to what extent the tectonic evolution of this region is controlled by subduction of the Nazca ridge and Inca plateau. A better understanding of the tectonic control of the deformation in the region has important implications for hydrocarbon exploration in the surrounding Marañon and Ucayali basins. The origin of hydrocarbon-bearing subsurface structures in the region is directly related to the origin of the surface structures that divide these basins. Previous studies have targeted only the subsurface structures in the Marañon and Ucayali basins separately, creating isolated contour maps on either side of the surface structures. In this study, the surface and subsurface geologic structures were mapped to create a complete map centered at the main basin-dividing structure. Seismic sections were interpreted to determine synsedimentary patterns (i.e., growth strata, onlap geometries) that can provide evidence of the time of uplift of the structures.

Earlier work (Hermoza et al., 2005; Alvarez-Calderon, 2004; Gil, 2001; Wine et al., 2003) shows the existence of an uplift referred to as the Contaya arch that separates the Ucayali and Marañon basins. Baby et al. (1999) proposed that the arch is a single, broad, uplifted structure limited by opposite basement reverse faults originating from inversion tectonics that began in the Late Cretaceous. In contrast, we interpret the Contaya arch to be composed of distinct structures with different structural styles and uplifted at different geologic times: the Contamana high, Contaya high, and Moa divisor (fig. 2). The Contamana high and Moa divisor have only recently been uplifted to their present elevations, and the Contaya high is shown to be a Triassic-Jurassic structure that was

also recently reactivated in the Tertiary. The recent reactivation is likely the result of the onset of flat slab subduction associated with downgoing Nazca ridge and Inca plateau. We speculate that the pre-existing structures likely helped to focus the stresses in such a way to allow deformation significantly farther away from the trench than in the surrounding areas of this part of the Andean margin.

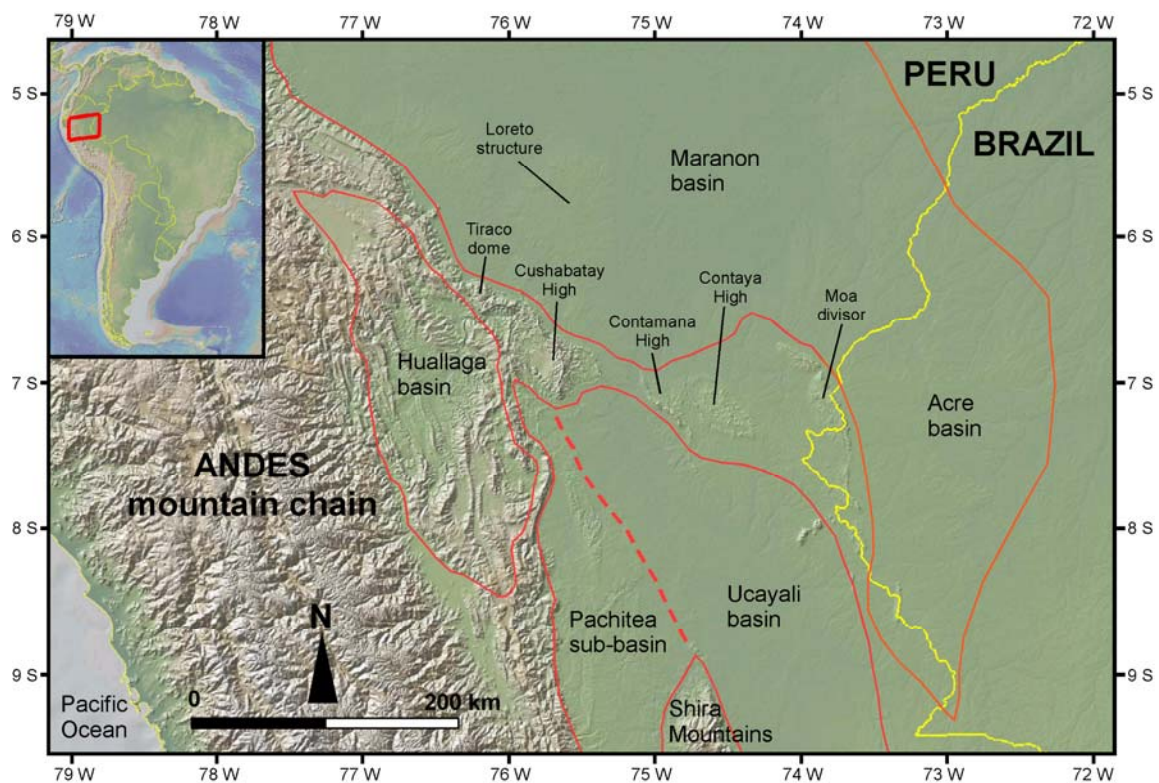


Figure 2. Location map showing the positive structures that divide the Marañon, Huallaga and Ucayali basins. Topography data from the Shuttle Radar Topography Mission (JPL NASA).

## **CHAPTER II**

### **BACKGROUND AND TECTONIC SETTING**

A synthesis of the tectonostratigraphic evolution of western South America between 5°S and 9°S has been compiled. First, we focus on the larger scale tectonic and geodynamic evolution as it relates to the major stratigraphic successions and regional unconformities that are observed in the Ucayali and Marañon basins. This is followed by a more detailed description of the stratigraphy of the basins affected by the uplifted structures examined in this contribution. Last, the most recent plate reconstruction models describing the subduction history of the Nazca plate are reviewed along with the effect of subduction of the Nazca ridge and Inca plateau on the deformation of the over-riding plate.

#### **Tectonic and geodynamic evolution of western South America**

Figure 3 shows a summary of the evolution of the region from Cambrian to the present based on Jacques (2004), Jaillard et al. (2002a), Aceñolaza (2002), Thomas (2002), Sempere et al. (2002), Jaillard and Soler (1996), Williams (1995), Gohrbandt (1992), Dalmayrac et al. (1988), Megard (1984) and Blakely (2008). The lithology in the stratigraphic column corresponds to the formations described in the Ucayali and Marañon basins.

During the Precambrian, western South America was most likely a divergent passive

margin that was part of the Gondwana supercontinent (Williams, 1997). By Cambrian to Silurian, a convergent plate boundary formed between the South American and the proto-Pacific plates, resulting in a back-arc extensional setting (Jaillard et al., 2002a) where the Contaya Formation marine shales and sandstones were deposited. The history of the margin from this point forward is dominated by convergent tectonics where both compressional and extensional regimes were locally important.

A transition from an extensional backarc system to a compressional retro-arc foreland system began in the Silurian and is marked by an erosional unconformity between the Contaya and Cabanillas Formation. The continent-continent collision between Laurentia and Gondwana from the Devonian to Permian would have influenced compressional deformational events in the study area. Of particular importance are the Eo-Hercynian and Juruá orogenies. As shown later, this deformation is observed in the seismic data where undifferentiated Devonian to Permian rocks form an anticline eroded by a Triassic unconformity.

During the Permian to Triassic, a transtensional rift developed, resulting in a series of grabens where the Mitu Formation continental red beds were deposited (Sempere et al., 2002). This rift episode was followed by regional thermal sag during the Triassic-Jurassic. Marginal marine shales and limestones were deposited at this time, forming the Pucara Formation. (Rosas et al., 2007). The deposition of these sediments was limited to the Marañón and Huallaga basins. During the Jurassic, a pre-Andean retro-arc foreland

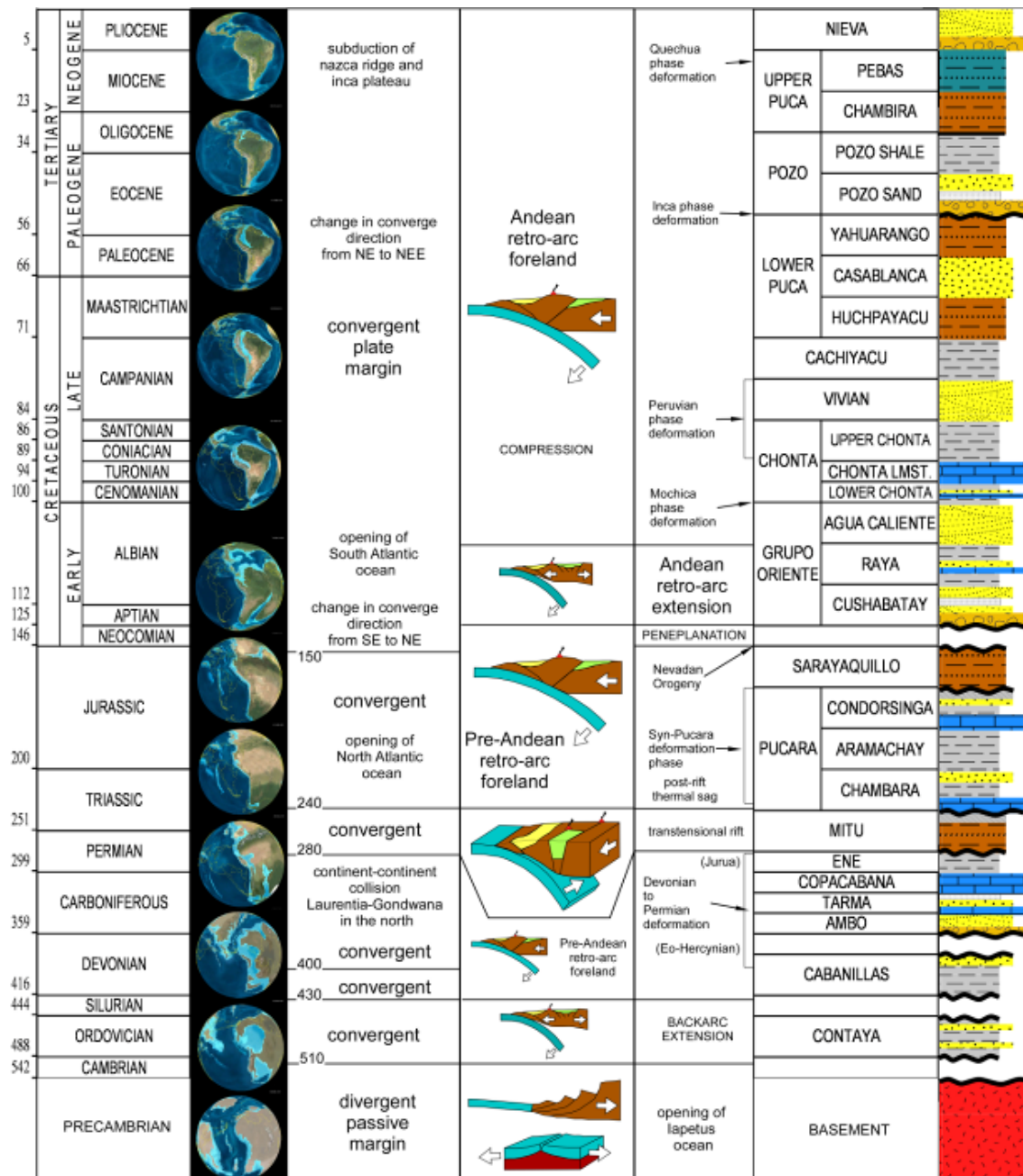


Figure 3. Tectonostratigraphic evolution of the Western border of South America between 5 and 9 South. The lithology corresponds to the Ucayali-Marañon basin and the images of the paleogeographic globes were obtained from Blakey (2008).

system formed where the Sarayaquillo continental red beds were deposited as a product of the erosion of the rising Andean mountain chain along the western border of South America.

A hiatus of about 20 m.y. between the top of the Upper Jurassic Sarayaquillo Formation and the overlying Cretaceous succession resulted from regional peneplanation. The base Cretaceous unconformity is related to the Nevadan Orogeny and to a major change in the convergence direction of the subducting Nazca plate (Jaillard et al., 2002a). Beginning in the Albian, the main compressional phases that uplifted the Andes mountain range began. The four most significant phases are the Mochica (Albian), the Peruvian (Santonian-Campanian), the Inca (Eocene), and finally the Quechua (Miocene), all of which are well documented in the literature (Jaillard et al., 2002a; Jaillard and Soler, 1996; Dalmayrac et al., 1988; Megard, 1984).

### **Stratigraphic evolution of the Marañon and Ucayali basins**

The Marañon, Huallaga and Ucayali basin share a similar sedimentary fill that ranges from Ordovician to Recent in age (fig. 4). They are separated from one another by the Cushabatay high, the Contamana high and the Contaya high. The geological evolution of the Ucayali and Marañon basins is usually divided into two systems in accordance with the preceding tectonic evolution, referred to as the pre-Andean and Andean systems.



Figure 4. Stratigraphic column for the Huallaga, Marañon and Ucayali basins. Modified from Hermoza (2004), Hermoza et al. (2005), Gil (2001), Espurt et al. (2008). The Pucara and Sarayaquillo Formations are absent in the Ucayali basin. Color lines represent identified seismic horizons: Permian-Triassic unconformity (magenta), Top Pucara limestone (light blue), base Cretaceous unconformity (red), Chonta limestone (green) Pozo sand (orange).

		Age	Huallaga basin		Maranon basin		Ucayali basin		lithology							
TERTIARY	NEOGENE	5	CONTAMANA GROUP	IPURURO	MARANON		TIMPIA									
		23		MIOCENE	UPPER PUCA	PEBAS	UPPER PUCA	IPURURO								
		34		OLIGOCENE	CHAMBIRA	CHAMBIRA	CHAMBIRA	CHAMBIRA								
	PALEOGENE	EOCENE	34	POZO	POZO SHALE	POZO	POZO SHALE	POZO	POZO SHALE							
			56		POZO SAND	POZO SAND	POZO SAND	POZO SAND								
		66	PALEOCENE	LOWER PUCA	YAHUARANGO	LOWER PUCA	YAHUARANGO	LOWER PUCA	YAHUARANGO							
	CRETACEOUS	LATE	MAASTRICHTIAN	LOWER PUCA	CASABLANCA	LOWER PUCA	CASABLANCA	LOWER PUCA	CASABLANCA							
					71	HUCHPAYACU	HUCHPAYACU	HUCHPAYACU	HUCHPAYACU							
					84	CACHIYACU	CACHIYACU	CACHIYACU	CACHIYACU							
		EARLY	CAMPANIAN	CACHIYACU	CACHIYACU	CACHIYACU	CACHIYACU	CACHIYACU	CACHIYACU							
86											VIVIAN	VIVIAN	VIVIAN	VIVIAN		
89			SANTONIAN	UPPER CHONTA	UPPER CHONTA	UPPER CHONTA	UPPER CHONTA									
94			CONIACIAN	UPPER CHONTA	UPPER CHONTA	UPPER CHONTA	UPPER CHONTA									
EARLY		TURONIAN	CHONTA	CHONTA LMST.	CHONTA	CHONTA LMST.	CHONTA	CHONTA LMST.								
										100	GENOMANIAN	LOWER CHONTA	LOWER CHONTA	LOWER CHONTA	LOWER CHONTA	
		ALBIAN	GRUPO ORIENTE	AGUA CALIENTE	RAYA	GRUPO ORIENTE	RAYA	GRUPO ORIENTE	RAYA							
	112										CUSHABATAY	CUSHABATAY	CUSHABATAY	CUSHABATAY		
125	APTIAN	CUSHABATAY	CUSHABATAY	CUSHABATAY	CUSHABATAY	CUSHABATAY	CUSHABATAY									
146	NEOCOMIAN	CUSHABATAY	CUSHABATAY	CUSHABATAY	CUSHABATAY	CUSHABATAY	CUSHABATAY									
JURASSIC	SARAYAQUILLO	SARAYAQUILLO	SARAYAQUILLO	SARAYAQUILLO	SARAYAQUILLO	SARAYAQUILLO	SARAYAQUILLO	SARAYAQUILLO								
										200	CONDORSINGA	CONDORSINGA	CONDORSINGA	CONDORSINGA	CONDORSINGA	
										251	PUCARA	ARAMACHAY	PUCARA	ARAMACHAY	PUCARA	ARAMACHAY
TRIASIC	CHAMBIRA	CHAMBIRA	CHAMBIRA	CHAMBIRA	CHAMBIRA	CHAMBIRA	CHAMBIRA									
PERMIAN	MITU	MITU	MITU	MITU	MITU	MITU	MITU									
CARBONIFEROUS	ENE	ENE	ENE	ENE	ENE	ENE	ENE	ENE								
										299	COPACABANA	COPACABANA	COPACABANA	COPACABANA	COPACABANA	
										359	TARMA	TARMA	TARMA	TARMA	TARMA	
DEVONIAN	AMBO	AMBO	AMBO	AMBO	AMBO	AMBO	AMBO									
416	DEVONIAN	CABANILLAS	CABANILLAS	CABANILLAS	CABANILLAS	CABANILLAS	CABANILLAS									
444	SILURIAN	CABANILLAS	CABANILLAS	CABANILLAS	CABANILLAS	CABANILLAS	CABANILLAS									
488	ORDOVICIAN	CONTAYA	CONTAYA	CONTAYA	CONTAYA	CONTAYA	CONTAYA									
542	CAMBRIAN	CONTAYA	CONTAYA	CONTAYA	CONTAYA	CONTAYA	CONTAYA									
PRECAMBRIAN	BASEMENT	BASEMENT	BASEMENT	BASEMENT	BASEMENT	BASEMENT	BASEMENT									

The pre-Andean system, which is dominated by the Eo-Hercynian and Jurua orogenic events, encompasses five stratigraphic successions of Ordovician (Contaya Fm.), Devonian (Cabanillas Fm.), Carboniferous to Permian (Ambo Fm., Tarma Fm., Copacabana Fm. and Ene Fm.), Permian-Triassic (Mitu Fm.) and Triassic-Jurassic ages (Pucara Group and Sarayaquillo Fm.) that overly the Precambrian basement of the Guyana and Brazilian Shields (Jaillard et al., 2002a). The boundary between the pre-Andean and the Andean system deposits is marked by a regional unconformity easily identified in the seismic sections and referred to as the base Cretaceous unconformity.

The Andean System encompasses two stratigraphic successions. The first is of Aptian-Miocene age (Grupo Oriente, Chonta Fm., Vivian Fm., Cachiyacu Fm., Lower Puca group and Pozo Fm.) and the second is of Miocene age to the present (Chambira Fm, Ipururo Fm. and Pliocene formations). The Aptian-Miocene succession forms a westward-thickening wedge of marine to fluvial clastic sedimentary rocks that make up the Chonta and Pozo Formations. Both generate strong reflections that are easily identified on seismic sections and can be tied to wells to provide regional correlation horizons. The term 'Andean' indicates that these sediments were deposited during the uplift of the Andes mountain chain along the Western border of South America.

The basement comprises upper pre-Cambrian igneous and metamorphic rocks that crop out on the eastern flank of the Shira Mountains (Megard, 1979). The earliest Paleozoic rocks deposited over this basement are the organic-rich shales and sandstones of the

Ordovician marine Contaya Group (Mathalone and Montoya, 1995). Little Silurian deposition or erosion is thought to have occurred (Mathalone and Montoya, 1995), and a thick coarsening-upward sequence of turbidites to deltaic sandstones from the Cabanillas Formation overlies the Ordovician rocks with an angular unconformity (Mathalone and Montoya, 1995; Espurt et al., 2008).

The Carboniferous to Permian sedimentary rocks of Ambo, Tarma, Copacabana and Ene Formations form a succession of rocks that is well known in the Peruvian basins. The lowest formation in this succession is the Ambo Formation, comprising conglomerates, sandstones, shales, coals, and subordinate tuffs (Newell et al., 1953). The Ambo Formation is overlain by the Tarma Formation, a thin cover of green sandstones, carbonates and local tuffs (Dunbar et al., 1946). These terrigenous strata are followed by the thicker fossiliferous platform carbonates of the Copacabana Formation (Cabrera La Rosa and Petersen, 1936). The Copacabana Formation is overlain conformably by black organic-rich shales and dolomites of the Ene Formation (Mathalone and Montoya, 1995; Espurt et al., 2008).

The continental and volcanic deposits of Mitu Formation consist of a succession of red to purple conglomerates, sandstones and shales interbedded with volcanic rocks. The Mitu Formation accumulated in isolated grabens that formed as a result of large scale extension, rifting and associated volcanism during the Permian-Triassic (Megard, 1979; Dalmarayac et al., 1988; Sempere et al., 2002).

Post-rift thermal subsidence resulted in the Pucara group, which consists of three separate formations, the Chambara, the Aramachay and the Condorsinga (Szekely and Grose, 1972; Rosas et al., 2007). The Chambara Formation is predominantly dolomitic with locally interbedded calcareous dolomites and limestones; the Aramachay Formation is dominated by black argillaceous limestones and shales deposited in a deep marine environment; and finally the Condorsinga Formation consists of limestones deposited in a carbonate platform environment. The top of Pucara sequence is marked by sabkha deposits (evaporites) identified in outcrops and in the subsurface by drilling and seismic data (Wine et al., 2001; Fernandez et al., 2002). The Pucara group is covered by the Sarayaquillo Formation, which consists of continental fluvial deposits (Tschopp, 1953; Megard, 1979).

The boundary between the pre-Andean system rocks (Ordovician to Jurassic) and the Andean system rocks (Cretaceous and Tertiary) is a regional unconformity that can be traced in the seismic sections along all of the sub-Andean basins of Peru and Ecuador. It is typically referred to in the literature as the base Cretaceous unconformity (Jaillard and Soler, 1996; Jaillard et al., 2002b; Mathalone and Montoya, 1995). This major regional unconformity is a result of the Nevadan orogeny and corresponds to a major change in the convergence direction in the late Jurassic - Early Cretaceous (Jaillard et al., 2002a; Jaillard et al., 1990). The lowermost Cretaceous unit is the Cushabatay Formation, which is composed of coarse-grained cross-bedded fluvial-deltaic sandstones. Overlying this are Albian organic-rich marine shales of the Raya Formation followed by the Agua

Caliente Formation, which signals a return to cross-bedded fluvial sandstones.

The Chonta Formation is composed of organic rich fossiliferous shales and limestones deposited in a transgressive marine environment (Kummel, 1948). The Chonta limestone generates a strong reflection in the seismic data that can be traced to the surface in the uplifted structures that divide the Marañon and Ucayali basins. Outcrops of Chonta limestone were mapped by INGEMMET (Instituto Nacional Geologico, Minero y Metalurgico del Peru) in the Contaya high, Cushabatay high and Moa divisor and can be identified on satellite images because of its strong resistance to erosion compared to the overlying and underlying shale deposits. Overlying the Chonta Formation are fluvial sandstones of the Vivian Formation (Seminario and Guizado, 1976) followed by shale deposits of the Cachiyacu Formation. These rocks represent the most important reservoir and seal rocks in the Marañon and Ucayali basins.

The Lower Puca and Upper Puca group are a thick, up to 1200 m, interval (Mathalone and Montoya, 1995) of red mudstones and sandstones deposited in an extensive alluvial plain and fluvial environment that covered most of the Marañon and Ucayali basins. These rocks act as the overburden required for the generation of hydrocarbons in the underlying Cretaceous and Paleozoic source rocks (Navarro et al., 2005). After the Middle Eocene, subsidence in the Marañon and Ucayali basins originated a marine incursion and the deposition of the Pozo Formation. The Pozo sand is observed as a strong reflection in the seismic data.

During the Miocene, at 10 Ma, an important tectonic event referred as the Quechua phase deformation (Megard, 1984) was responsible for the reactivation and uplift of the structures that divide the Marañon and Ucayali basins, giving them their present day configuration. For this reason the Late Miocene-Pliocene deposits in these basins represent two different isolated formations; Pebas-Marañon Formation in the Marañon basin and Ipururo-Timpia Formation in the Ucayali basin.

### **Subduction of the Nazca ridge and Inca plateau**

There are two important topographic features on the downgoing plate that are thought to have had a significant impact on deformation of the overriding plate. To the south of the study area is the Nazca ridge and to the north is the Inca plateau.

The Nazca ridge is a more than 1000 km long, 200 km wide and 1.5 km high aseismic submarine ridge that formed at the Pacific Farallon/Nazca spreading center in the early Cenozoic (Hampel, 2002). A number of features in the offshore and onshore geology of the Peruvian margin, such as uplift and subsidence of forearc basins, tectonic erosion of the lower continental slope and uplift of marine terraces have been attributed to ridge subduction. In addition, the downward continuation of the ridge has been related to a zone of reduced intermediate depth seismicity and to the southern boundary of the low-angle subduction segment beneath Southern Peru (Hampel, 2002). Because the ridge is oblique with respect to both the strike of the trench and the convergence direction

between the Nazca Plate and South American plates, it migrates southward along the active plate boundary. As a result, the effects of the ridge subduction also appear to migrate from north to south (Hampel, 2002).

Hampel (2002) reconstructed the migration history of the Nazca ridge using updated plate motion data. His model suggests that the component of ridge motion parallel to the margin decreased in velocity from 75 mm/a before 10.8 Ma, to 61 mm/a from 10.8-4.9 Ma, and then to 43 mm/a from 4.9 Ma to the present. Since the length of the original Nazca ridge can be determined by its conjugate feature on the Pacific Plate (the Tuamotu Plateau), Hampel estimated that an approximately 900 km long segment of the Nazca ridge has already been subducted. From this and from the plate reconstructions, Nazca ridge subduction began at 11.2 Ma at a location  $\sim 11^\circ\text{S}$ . While the existence of the Nazca ridge is beyond doubt, the second important feature, the Inca plateau, is more speculative. Gutscher et al. (1999) propose that an oceanic plateau was formed at the East Pacific Rise as the mirror image of the Marquesas Islands 45–50 Ma ago. He named this the Inca plateau and showed that if it existed, it subducted beneath northern Peru 10–12 Ma ago.

Both of these features would be expected to be positively buoyant compared to normal oceanic crust. Thus, they will be difficult to subduct, providing a simple mechanism to explain why the slab appears to flatten out beneath the South American plate between  $5^\circ$  and  $9^\circ$  S. In essence, the 1500 km long Peruvian flat slab portion of Nazca Plate is



supported by two buoyant bodies, Nazca ridge to the South and Inca plateau to the North, with intervening sag. This general model is supported by most recent work, although many details, in particular the timing of events, remain uncertain. For example, Rosenbaum et al. (2005) showed that ridge subduction may have played a role in triggering the Miocene episode of magmatic–hydrothermal metallogenic activity in the Peruvian Andes.

Rosenbaum's kinematic reconstruction (fig. 5) shows that the subduction of the Nazca ridge and the Inca plateau is temporally and spatially related with metallogenic and volcanic activity on the overriding South America plate from 16 Ma to present. According to this reconstruction (Rosenbaum et al., 2005), the tip of the Nazca ridge began to interact with the subduction zone at 16 Ma (fig. 5 g), earlier than the 11.2 Ma age suggested by Hampel (2002). At 10 Ma the whole length of the Inca plateau (150–250 km) had already been consumed at the subduction zone and the tip of the subducted Nazca ridge was located beneath the Ucayali basin (fig. 5 j).

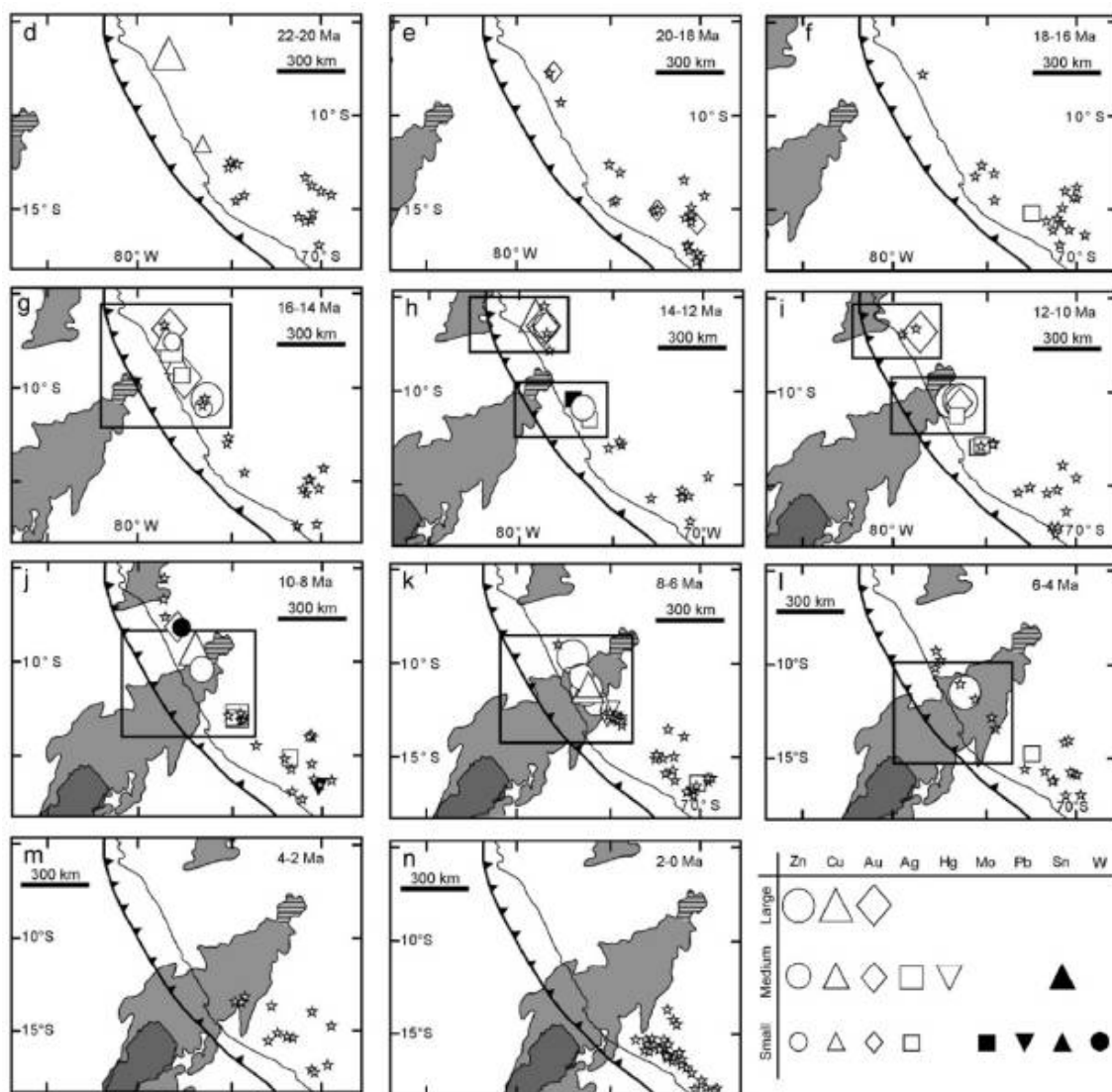


Figure 5. Reconstruction of the subduction history of Nazca ridge and Inca plateau. From Rosenbaum et al. (2005). The Nazca ridge and Inca plateau are shown in grey. Symbols represent ore deposits and volcanic centers in the Peruvian Andes. In this reconstruction, Nazca ridge subduction started at 16 Ma and the tip of the subducted Nazca ridge was located beneath the Ucayali basin in the Miocene at 10 Ma.

### CHAPTER III

#### DATA AND METHODS

To better understand the uplifted features of the Contaya arch and their timing relative to the major tectonic events in the region, we examined regional geophysical and geological datasets available. These data include surface geologic maps published by INGEMMET at scale 1:100000, Landsat ETM+ satellite imagery, SRTM digital elevations models, regional 2D seismic grids provided by Perupetro, and GR-SP-Resistivity logs from wells in the Marañon and Ucayali basins (Table 1).

Table 1. Wells used in this study.

Platanal 1X	Pacaya 31X	Santa Lucia 2X
Sanuya 3X	Amaquiria 32X	La Frontera 3X
Rio Caco 4X	Cachiyacu 1X	Palmera 4X
Tamaya 2X	Maquia 1X	Tamaco 1X
Tiruntan 1X	Insaya 1X	Palo Seco 1X
Cashiboya 29X	Huaya 3X	Viracocha 2X
Cashiboya 1	Santa Clara 1A	Pauyacu 1X
Inuya 1	Orellana 3X	Loreto 1X
Pacaya 1	Santa Catalina 2X	Shanusi 2X

The 2D seismic data consists of 20 surveys covering the Ucayali basin and 12 surveys covering the southern Marañon basin recorded between 1973 and 1998 (fig. 6). These data sets were post-stack time migrated by Perupetro and delivered in SEG-Y format.

The quality of the 2D regional lines is sufficient to trace the horizons throughout the region. In some areas, corrections (small shifts) were required to ensure that all data is referenced to the same datum. Some of the older seismic lines were only available on paper sections and were digitized and converted to SEG-Y files by Perupetro. In this research, all the seismic lines located in the Ucayali and Marañon basins (fig. 6), totaling more than 200 lines, were interpreted.

In addition to the seismic reflection grid, more than 50 exploration wells have been drilled in the Ucayali and Marañon basins in the 80's and 90's. The GR, SP and resistivity logs from these wells were provided by Perupetro in LAS files. Some wells also included sonic, neutron and density logs.

Formation tops were identified in wells located in the Marañon and Ucayali basins using the information from final well reports, well logs (GR, SP and resistivity) and published cross sections. These were then tracked and correlated in a regional north to south 1200 km long cross section across the Contaya high and includes wells from both basins (fig. 7). Because of the varying vintages of data, seismic sources, and processing, detailed well ties from synthetic seismograms proved to be a very difficult exercise. However, the goal of the mapping is to establish regional, large scale patterns, so misties on the order of 10-100 msec are of no consequence to the overall goal and mapping exercise. Correlations to the wells were done by identifying key horizons and reflection patterns in the available data reports (Wine et al., 2002, 2003) and checking that the time intervals

between picked horizons matched and that the seismic responses were similar.

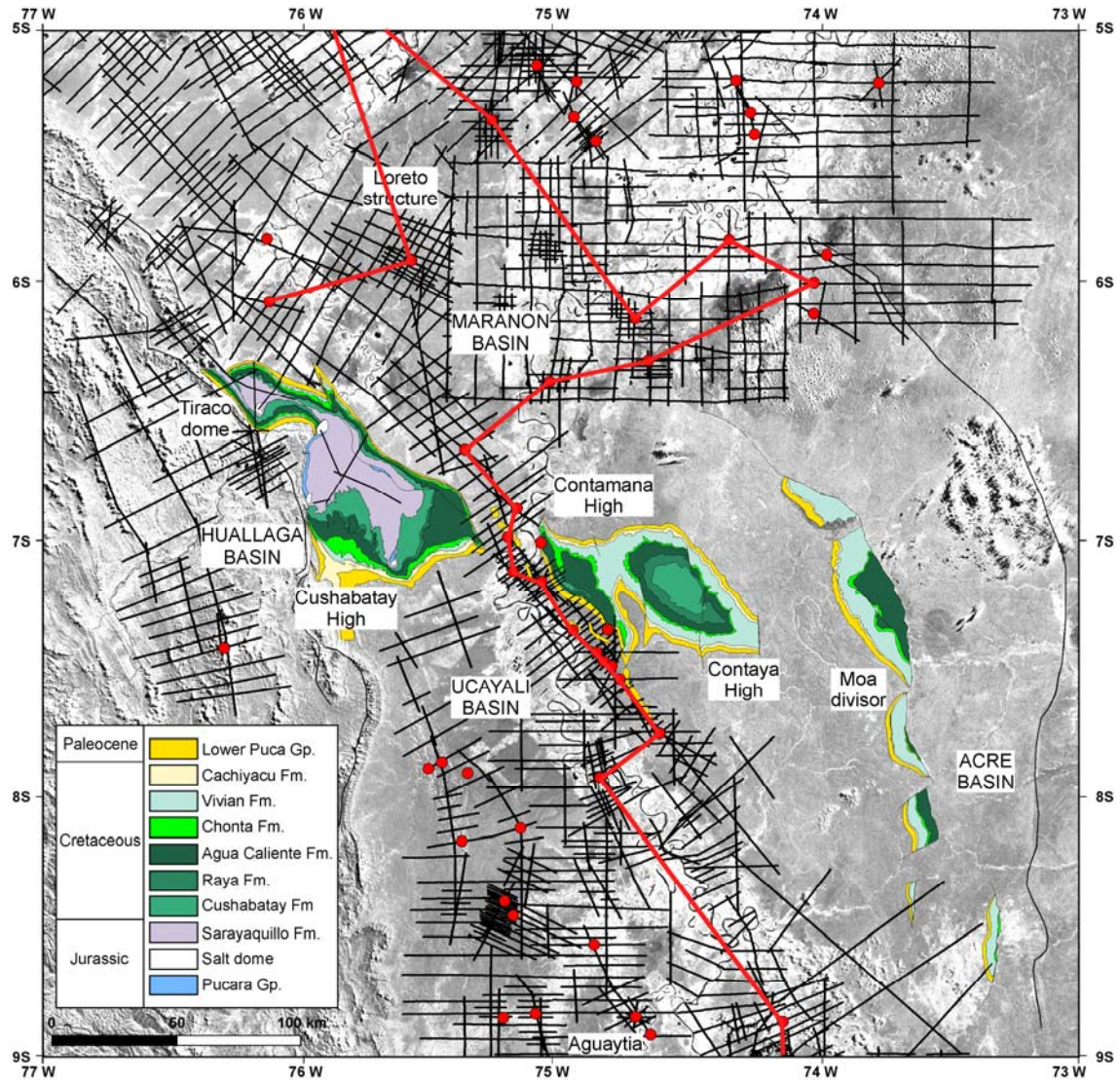


Figure 6. Grayscale satellite image (Landsat ETM+) showing the interpreted 2D seismic lines (black lines) and wells used in this study (red dots). Red line represents the well correlation shown in detail in figure 7. Surface geology from INGEMMET.

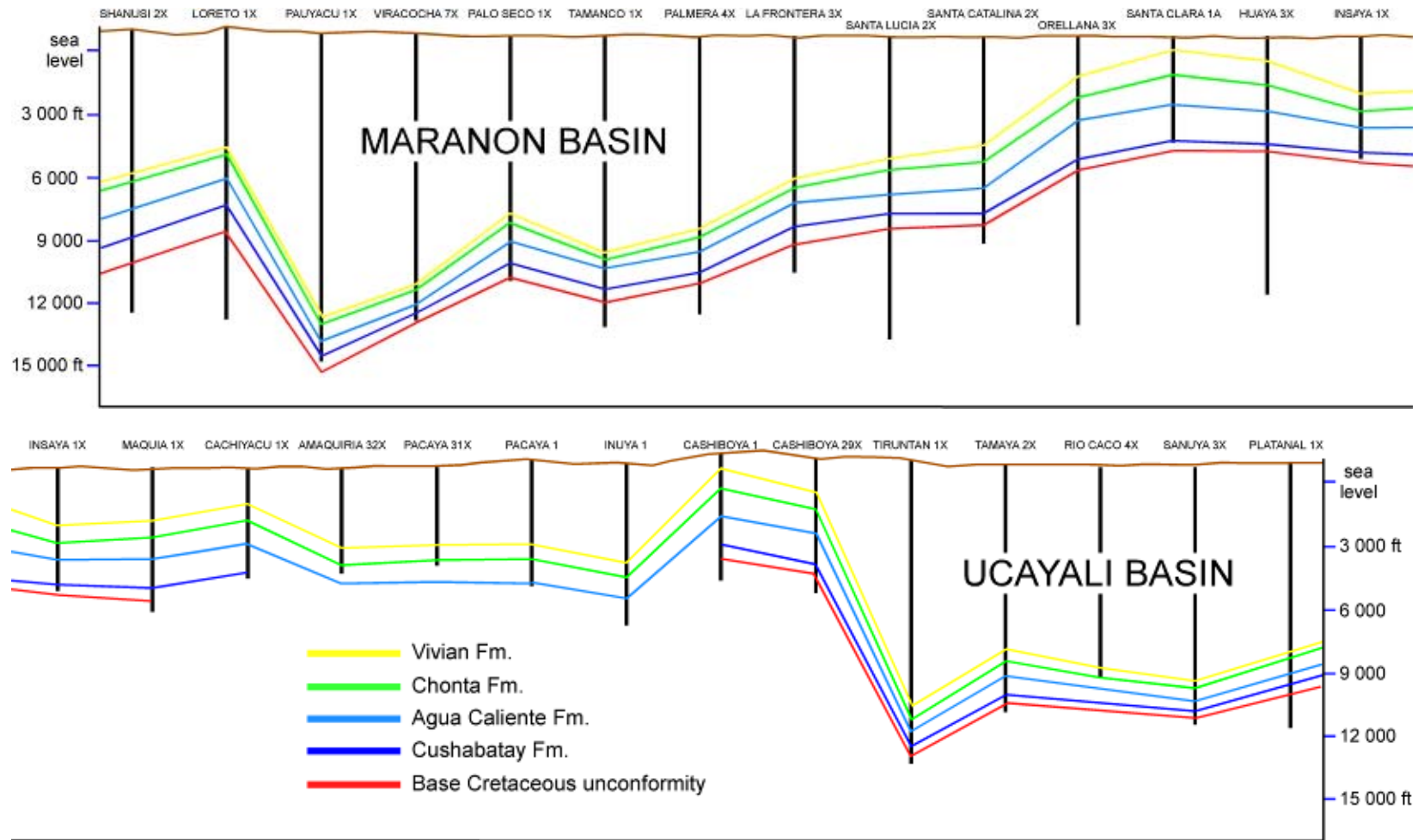


Figure 7. Regional well correlation. Image is split in two panels to ensure it is legible. Cross section with equally spaced wells.

To establish the relative timing of different compressive events, five key seismic horizons were identified and mapped. From oldest to youngest, these are the top Mitu or base Pucara Formation (Permian-Triassic unconformity), the top Pucara limestone (Jurassic), the base Cushabatay Formation (base Cretaceous unconformity), the top Chonta limestone (late Cretaceous), and the base Pozo sandstone (Eocene). All but the last are strong continuous reflections and were relatively easy to follow through the seismic sections once the well correlation was established. Identified packages of similar seismic facies between the horizons were used to determine if the horizons were correctly picked.

The deepest reflection mapped regionally is a Triassic unconformity that marks the base of the Pucara Formation or top of Mitu Formation (magenta horizon). This unconformity marks the transition from a transtensional rift setting (Mitu Fm.) to a post-rift thermal sag setting (Pucara Fm.). In many parts of the basin Ordovician to Permian age strata are erosionally truncated by this unconformity, providing evidence for Paleozoic deformation.

The top Pucara limestone (light blue horizon) is a relatively strong continuous reflection due to the large acoustic impedance contrast between the Pucara limestone and the underlying Aramachay shale. The Pucara Formation is not observed in the Ucayali basin and was only mapped in the Marañon basin and South from the Cushabatay high.

The base Cretaceous unconformity (red horizon) and the Chonta limestone horizon (green horizon) were the most clear to pick and both are the only two horizons present in all the seismic data. The base Cretaceous is a regional erosional unconformity that can be traced in the seismic sections along all of the sub-Andean basins of Peru and Ecuador. It is normally identified as a boundary between stratified sediments above that produce a well defined reflectivity pattern sub-parallel to the unconformity, and erosionally truncated and wedge-shaped sediments below.

The Chonta limestone horizon is a strong continuous reflection produced by the acoustic impedance contrast between the Chonta limestone and the overlying Upper Chonta shale. In many elevated regions it crops out and can be identified on satellite images as a thick, weather resistant, continuous layer. Because of this, it is possible to map this horizon in the elevated regions where no seismic profiles exist. To accomplish this, elevations of the Chonta limestone outcrops were obtained from the digital elevation models. These were then converted to two-way travel time referenced to the same datum used in the seismic sections assuming an average velocity of 1500 m/s, which is appropriate for highly weathered sedimentary rocks. The travel-times are subtracted from the datum so that negative values distinguish points mapped in elevated areas from those mapped in seismic sections.

The shallowest reflector mapped is the Eocene Pozo sand (orange horizon). This horizon was only mapped in areas with sufficient well control because it is not always easily



recognizable. This is either because it is not present, or because only a weak acoustic impedance contrast between the overlying and underlying shales does not always produce a clear reflection.

Confidently mapping fault surfaces in 3 dimensions on regional 2D seismic data is a difficult task. To get a basic overview of the structural fabric, we concentrated on mapping only the major unambiguous faults on the seismic sections. These were then correlated to their surface expression as observed in the satellite images and digital elevation models. Smaller scale structures are identified and mapped where they help to establish the timing of deformation relative to the mapped horizons, but we cannot always correlate these smaller structures from line to line with great confidence. The thinning of intervals against structures and the offset of horizons by reverse faults were used to determine the time of uplift of the structures identified in the seismic data.

.

## CHAPTER IV

### RESULTS AND DISCUSSION

By comparing the relationships between the mapped horizons and the major faults in the region, it is possible to establish when the various structures that compose the Contaya arch were formed. In this section we summarize the main evidence in the seismic data that demonstrates that the Contaya arch consists of three distinct structures that formed initially at different times and were recently reactivated. The structures that form the Contaya arch are: 1) NW-SE elongated structures bounded by high angle reverse faults inverted in the Tertiary: the Contamana high and the Moa Divisor. 2) Triassic-Jurassic structures: the Contaya high.

Seismic sections that show clear evidence of uplift and deformation at different geologic times were selected from all the interpreted seismic lines (fig. 8). To clearly see the structures and their inter-relationships, the profiles chosen (figures 9 to 13) are oriented nearly perpendicular to the main interpreted structures. Profile AA', located in the Marañon basin, relates to the Contaya high. Profiles BB' and DD' are related to other structures in the Ucayali basin that were formed by the same deformation events that originated the structures that compose the Contaya arch. These profiles are shown as supporting evidence of these deformation events. Profile CC' and EE' relate to the Contamana high and the Moa Divisor, respectively, as they cross the reverse faults that bound these structures.

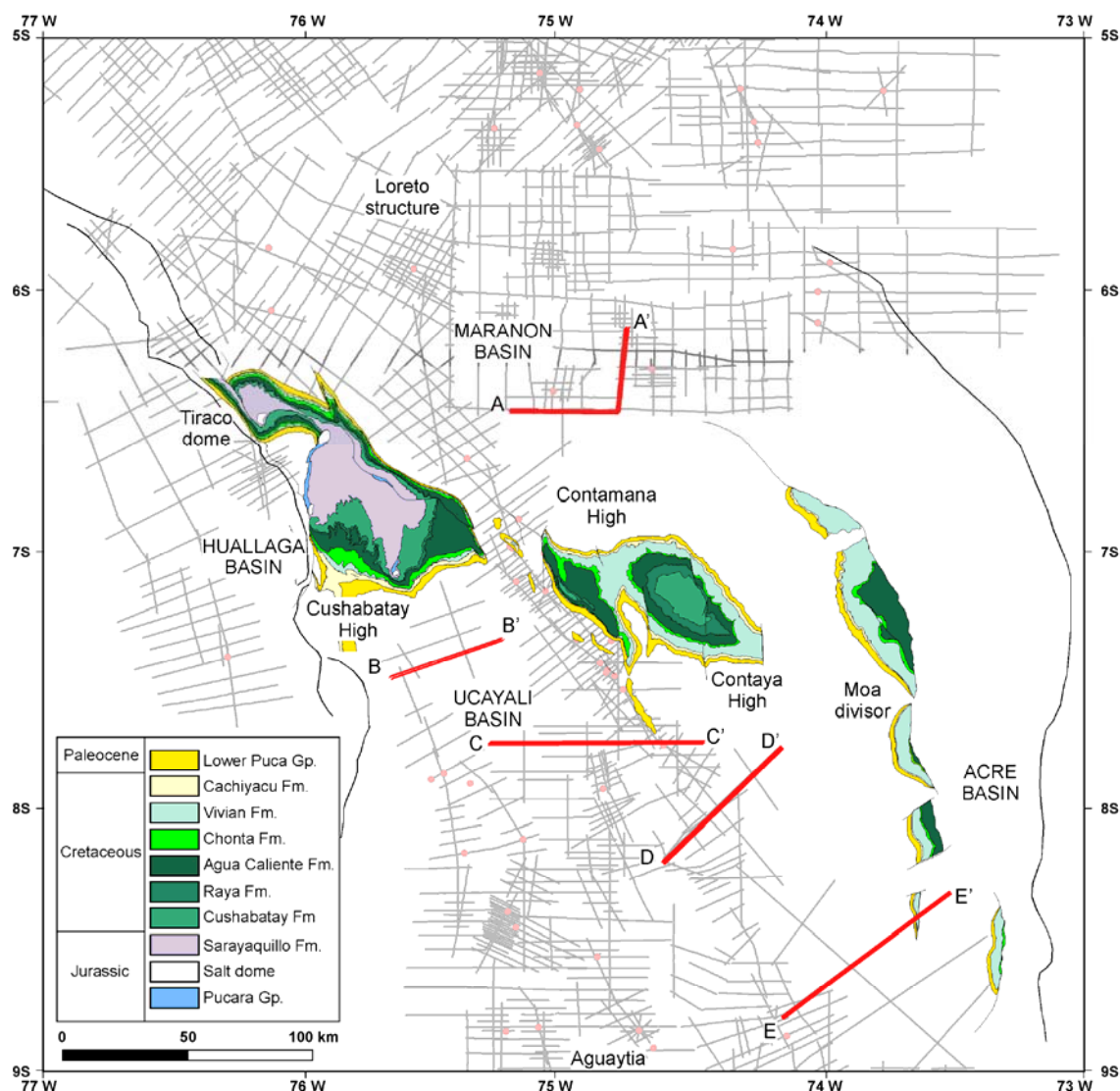


Figure 8. Seismic sections location map. Location of figures 9 to 13 is shown as red lines.

On seismic line B-B' (fig. 9), onlap of the Pucara Formation (light blue horizon) over base Triassic unconformity (magenta horizon) is evidence of a Triassic-Jurassic syn-Pucara deformation phase. Undifferentiated Devonian to Permian rocks and Mitu Formation deposits filling Permian-Triassic half grabens were uplifted in the Triassic-Jurassic during Pucara deposition. The normal faults bounding half-grabens were

reactivated into reverse faults, creating a positive topography that limited the deposition of Pucara Formation and associated salt deposits to the Huallaga basin and the Cushabatay high area in the west. This would further explain the absence of the Pucara Formation in the Ucayali basin. The Triassic unconformity marks the transition from a Permian-Triassic transtensional rift setting, evidenced by the half-grabens, to a Triassic-Jurassic post-rift thermal sag setting, evidenced by the onlap of Pucara Fm over the inverted structures. From Early Cretaceous to Tertiary the reverse faults remained inactive, as evidenced by the parallel reflectors above the base Cretaceous unconformity (red horizon), and finally were reactivated in the Tertiary (most probably in the Miocene). The Triassic-Jurassic deformation shown in profile BB' is also evidenced in profile AA', which is related later in the text to origin of the Contaya high.

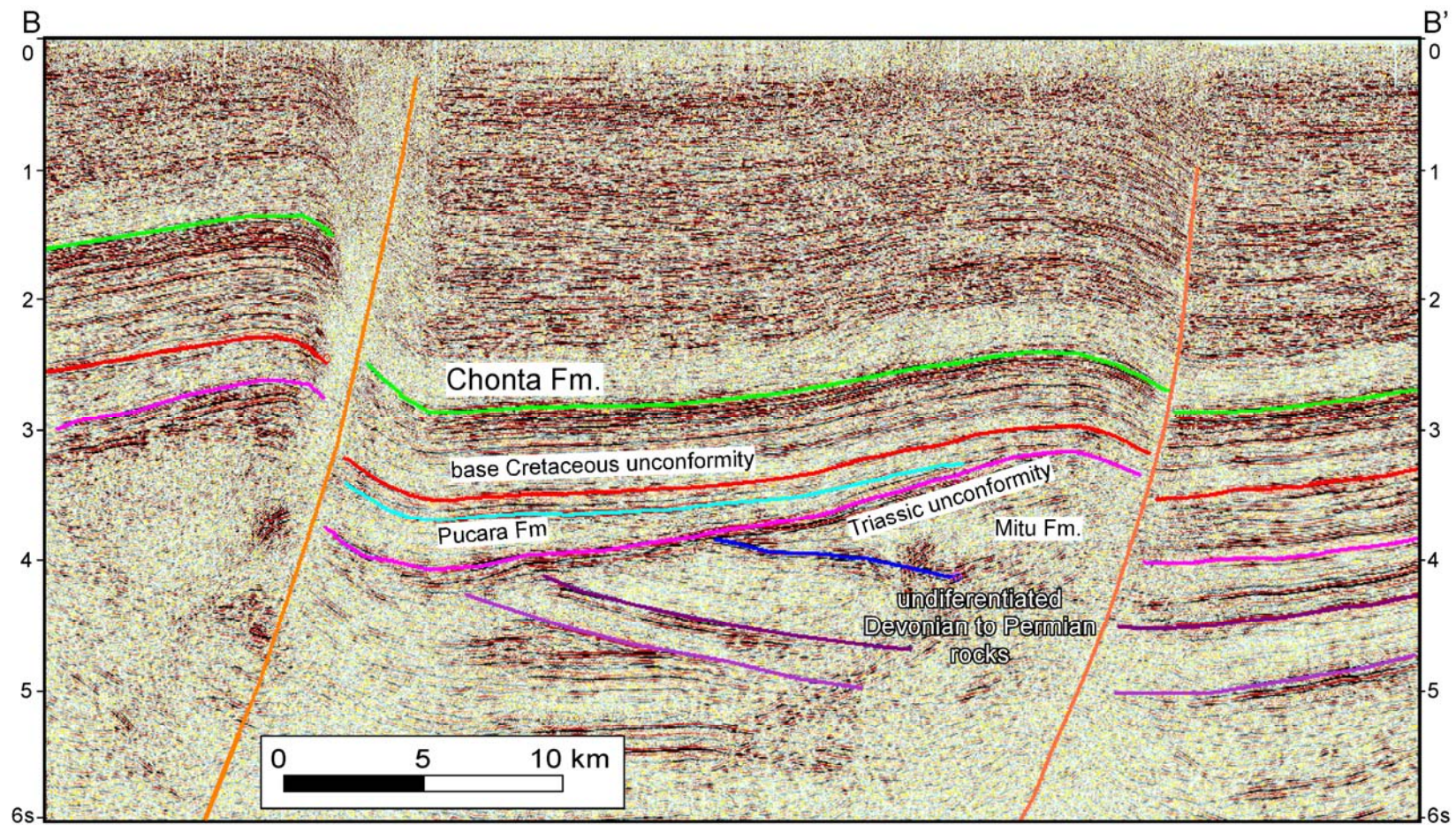


Figure 9. Seismic section BB'. See figure 8 for location. The onlap of Pucara Formation (blue horizon) evidences uplift of the structure during Pucara deposition (Triassic-Jurassic).

To the east, the origin of the Contamana high is most clearly demonstrated along seismic profile CC' (fig. 10). High angle reverse faults that bound the structure cut through the Cretaceous and Tertiary sedimentary rocks. The faults and consequent uplift are part of a retro-arc foreland setting after deposition of the Pozo Formation in the Eocene. Thus, the uplift of the Contamana high is clearly related to Andean subduction tectonics despite its unusual location well within the foreland basin.

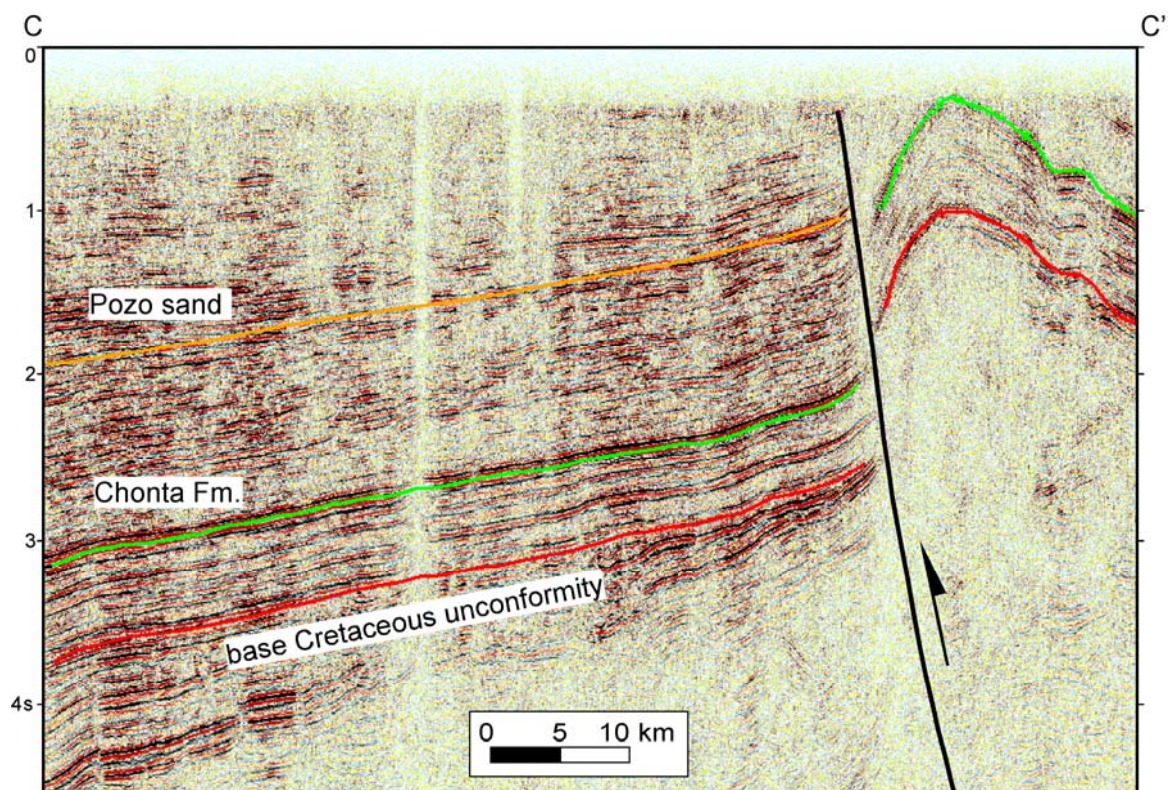


Figure 10. Seismic section CC'. See figure 8 for location. Tertiary deformation is evidenced by high angle reverse faults cutting through Cretaceous and Tertiary rocks.

The Moa divisor, which divides the Ucayali basin from the Acre basin in Brazil, is a positive structure bounded by a west dipping, thick skinned, high angle reverse fault (profile EE', fig. 11) that cuts through the Cretaceous and Tertiary sedimentary rocks and has a similar origin to the fault bounding the Contamana high (fig. 10). A half-graben filled with Mitu Formation rocks, is evidence that this fault originated as a normal fault in the Permian-Triassic transtensional setting described earlier. Since the fault cuts through the Cretaceous and Tertiary sedimentary rocks, it was reactivated as an inversion structure during Andean deformation in the Tertiary. Latrubesse and Rancy (2000) show the existence of a system of N-S reverse faults, located East from the Moa Divisor in the Acre basin, and relates their origin to the presence of a segment of low-angle subducting Nazca Plate at these latitudes.

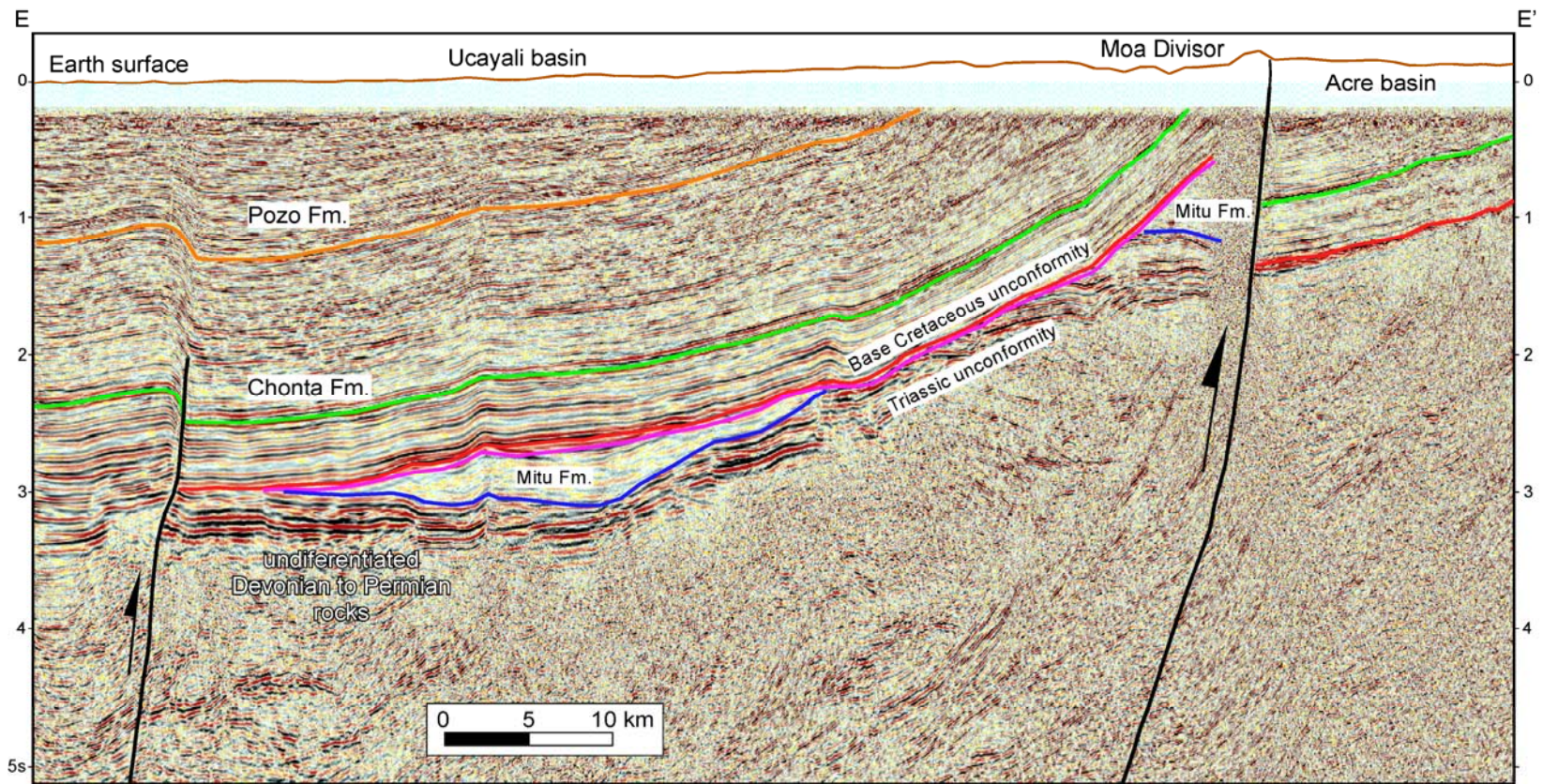


Figure 11. Seismic section EE'. Moa divisor and Mitu deposits. The Moa divisor is a Tertiary structure limited by a high angle reverse fault that cuts through the Cretaceous and Tertiary rocks. The Mitu Formation deposits are limited to transtensional grabens below the Triassic unconformity.



Evidence of Devonian to Permian deformation is observed on the seismic section DD' (fig. 12). Undifferentiated Paleozoic sedimentary rocks form an anticline structure that has been eroded and is capped by the Triassic unconformity (magenta horizon) and undeformed Cretaceous and Tertiary deposits (Chonta and Pozo horizons). This deformation would have taken place in a Devonian to Permian retro-arc foreland system and would correlate to the Eo-Hercynian and Jurua deformation phases described by Bump et al. (2008) and Rosas et al. (2007). The distribution of this Devonian to Permian structures in the Ucayali basin and their effect on younger structures (Contamana high, Contaya high and Moa Divisor) is not well understood because no other clear evidences of deformed pre-Mitu deposits have been found in the seismic data.

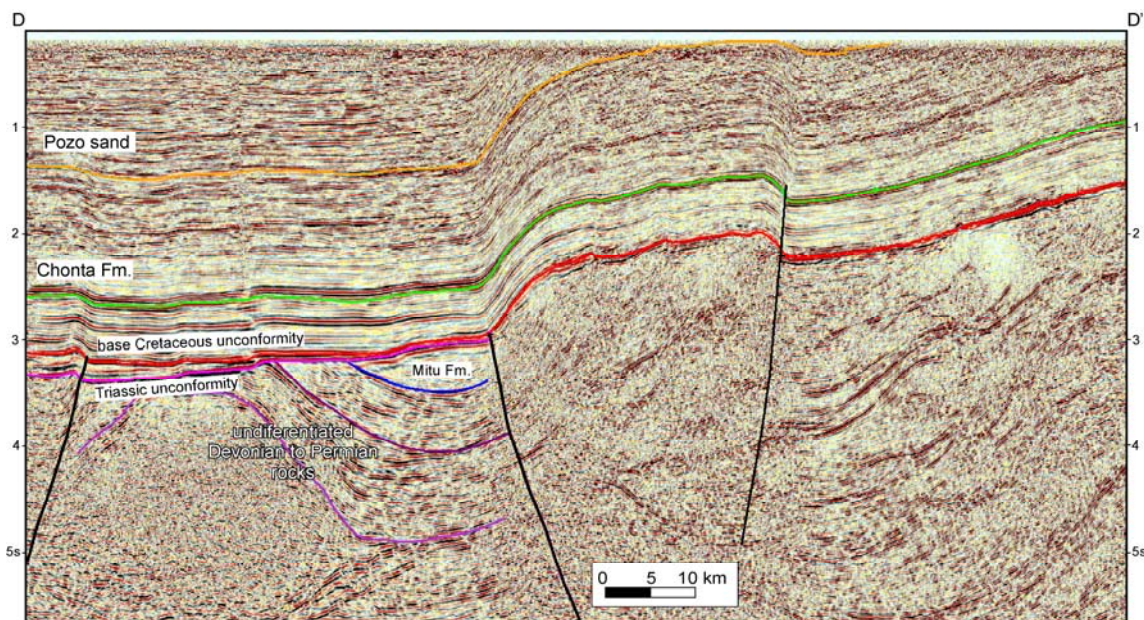


Figure 12. Seismic section DD'. Evidence of Devonian to Permian deformation correlated to the Eo-Hercynian and Jurua deformation. See figure 8 for location.

Finally, the Contaya high, which is located on the border between the Marañon and Ucayali basins, was uplifted in a retro-arc foreland tectonic setting during the Triassic-Jurassic as seen in the composite section AA' (figures 13 and 14). The Triassic-Jurassic Pucara Formation has been uplifted and subsequently eroded during the Neocomian peneplanation event that caused the base Cretaceous unconformity (red horizon). The fact that the overlying Cretaceous to Tertiary strata are not horizontal and have been deformed to a point in which the Chonta Formation crops out in the Contaya high, shows that this Paleozoic structure was reactivated in the Tertiary during the Andean deformation, most probably in the Miocene after Pozo Formation deposition as evidenced in the flattened seismic section AA' (fig. 14).

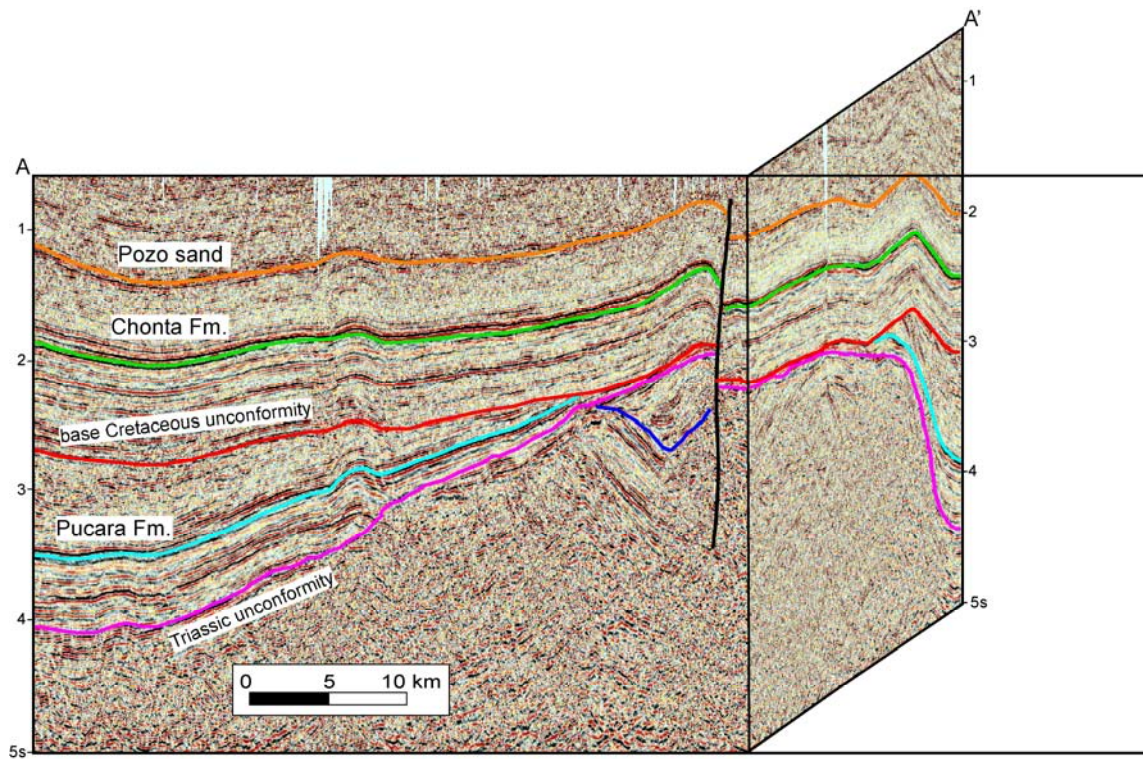


Figure 13. Seismic section AA'. This composite seismic section shows evidence of Paleozoic uplift for the Contaya high. The erosional truncation of the Triassic-Jurassic Pucara Formation against the base Cretaceous unconformity would be an evidence of uplift of the Contaya high in a compressive retro-arc foreland tectonic setting during the Triassic-Jurassic. The structure and the overlying Cretaceous and Tertiary rock were later deformed during the Tertiary probably in the Miocene during the last Andean deformation phase (Quechua phase). See figure 8 for location.

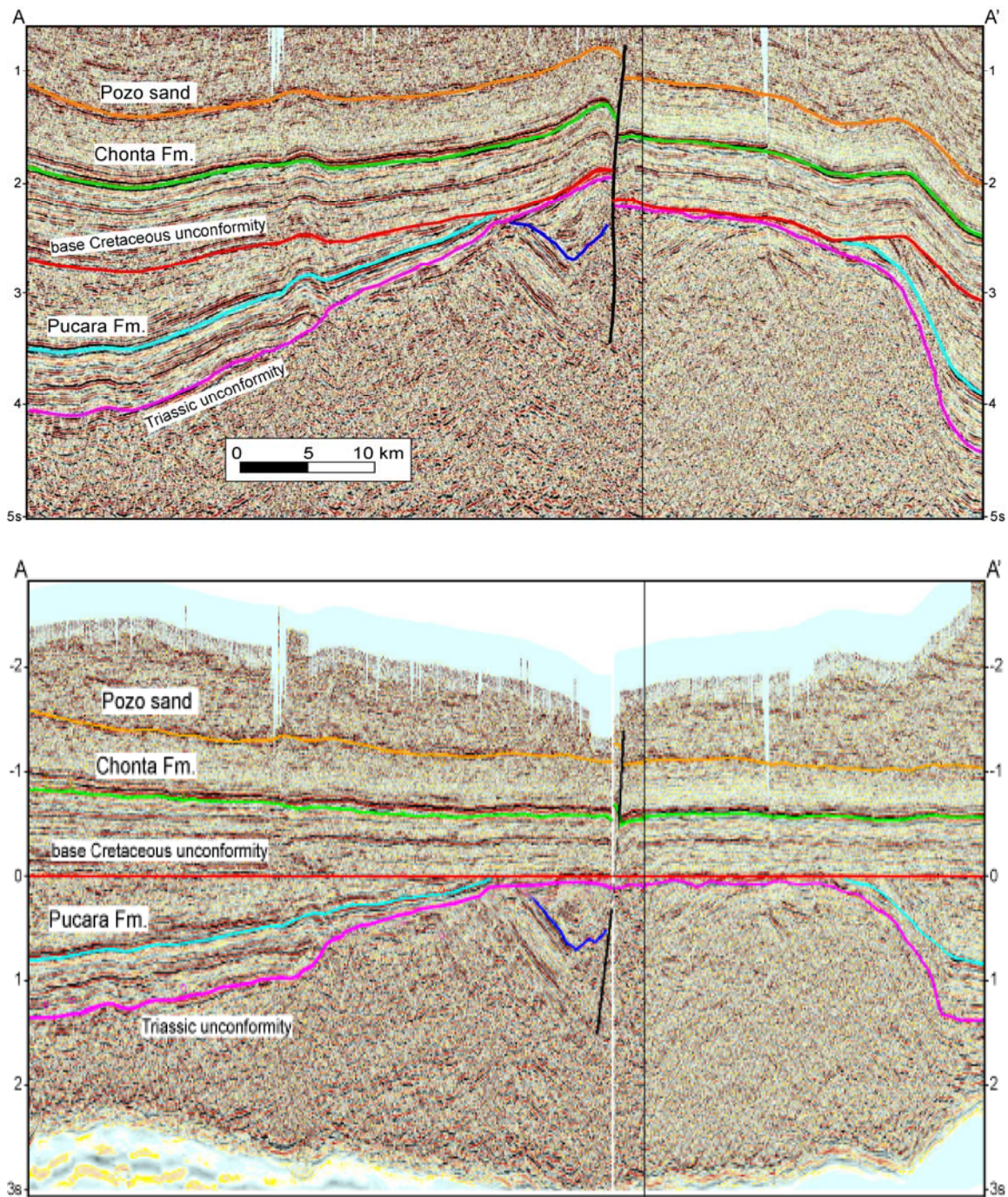


Figure 14. Seismic section AA' flattened at the base Cretaceous unconformity horizon. The flattened cross section shows that during the Neocomian, the Contaya high was a positive structure eroded by the base Cretaceous unconformity. The parallel reflectors in the Cretaceous and Tertiary section (between the red and orange horizon) indicates that the reactivation of the Contaya high occurred after Pozo Formation most probably in the Miocene.

Figure 15 shows a time structure map of the Chonta Formation horizon that summarizes some of the key issues raised by the detailed mapping shown above. It includes outcrop elevation points, converted to seconds as described in the previous section, where there is no seismic data. The resulting map is a seamless time structure map that shows the distribution of the Chonta Formation in the uplifted areas (negative points above zero seconds, colored in orange) and in the subsurface. The faults shown on this map are the faults observed on the seismic sections and their surface expression observed in the satellite images, digital elevation models and surface geology maps. The map highlights the fact that the Contaya arch is not a single structure, but instead it is composed of five different structures, the Tiraco dome, Cushabatay high, Contamana high, Contaya high and Moa divisor.

## **Discussion**

More than 200 regional 2D seismic lines covering an area close to 96 000 km<sup>2</sup> were interpreted with the objective to understand the origin of the structures that divide the Ucayali and Marañon basins. Interpreted regional faults and the patterns in relation to the major faults were analyzed to determine the time of uplift of the Contamana high, Contaya high and Moa divisor. The results show that the uplift of the Contamana high and Moa divisor and the reactivation of the Contaya high occurred in the Tertiary, most probably in the Miocene after Pozo Formation deposition. We suggest that reactivation is a result of subduction of the Nazca ridge.

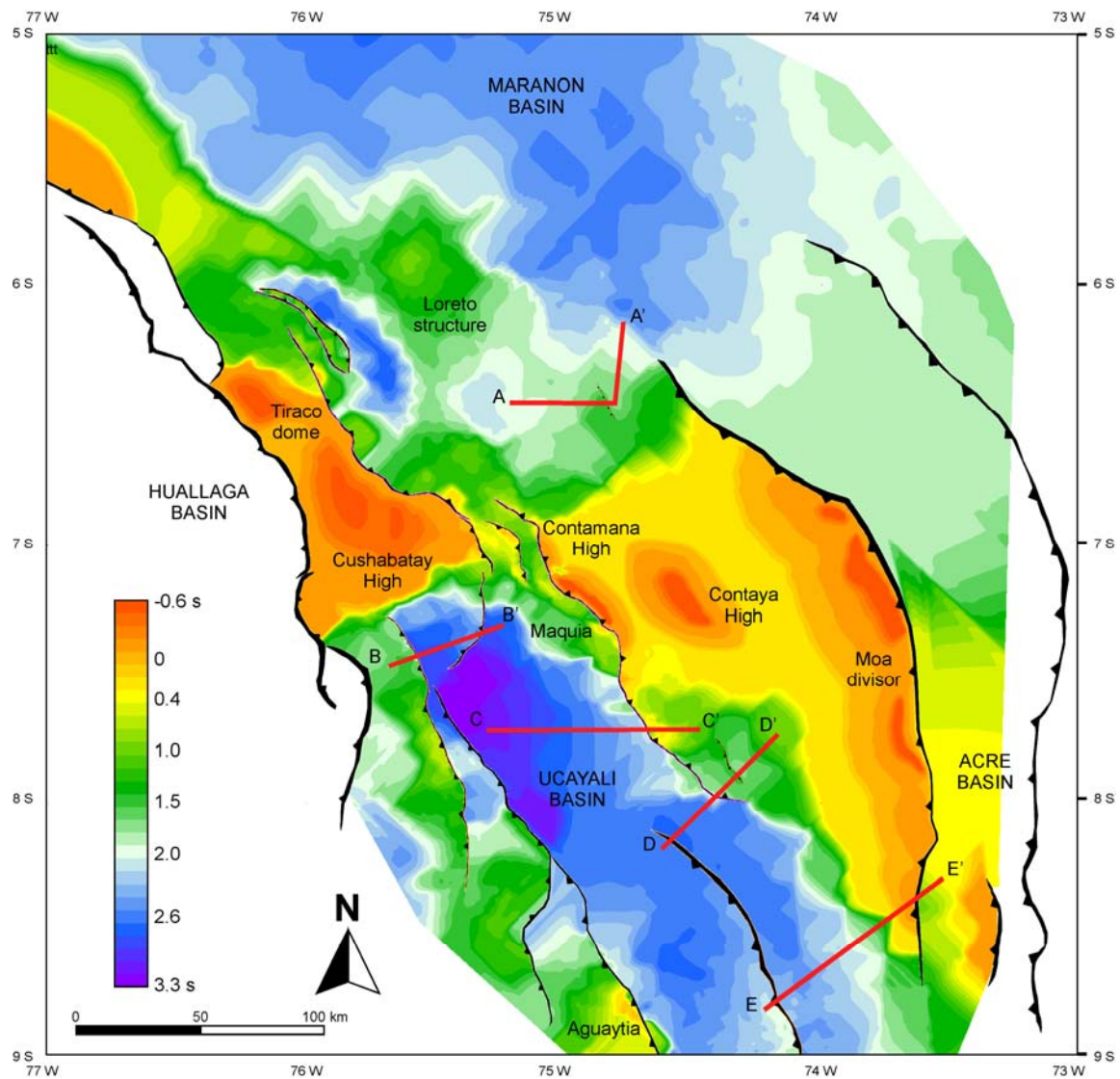


Figure 15. Time structure map at Chonta limestone horizon. Negative values above 0 seconds represent areas where the Chonta Formation is outcropping. Red lines represent the interpreted seismic sections. The uplifts that compose the Contaya arch are shown in orange as positive structures above the seismic datum.

The greater contact area between the plates and higher degree of interplate coupling produce greater crustal seismicity and higher magnitude stresses in the upper plate above flat-slab regions than over steep slab segments (Smalley et al., 1993). Focal mechanisms in the upper plate above flat slab segments are compressional (thrust type) to transcurrent (strike-slip) with P-axis aligned perpendicular to the trench, suggesting the subduction boundary stress is effectively transmitted to the upper plate (Gutscher, 2002). Increased interplate coupling above flat slab segments can be responsible for thick-skinned deformation in the upper plate. For example, it has been proposed that uplift of the Pampeanas Range in Argentina (Jordan et al., 1983) and large-scale block-type uplifts in the Eastern Cordillera in Colombia (Gutscher et al., 2000) are a result of such thick skinned tectonics. We propose that a similar mechanism produced compression and uplift of the Moa Divisor, the Contamana high and the reactivation of the Contaya high during the Tertiary in response to the flat slab subduction of the Nazca ridge and the Inca plateau.

Previous work along the Andean chain has overlooked this compressional deformation in Peru. Jordan (1983) compared the foreland deformation above segments of flat slab subduction in the Pampeanas range in Argentina and the Peruvian fold and thrust belt. She describes a less degree of foreland basement deformation in Peru compared to Argentina, attributed to the younger age of the flat slab subduction (5 Ma in Peru compared to 10-15 Ma in Argentina). Based on the seismic interpretation and detailed mapping from this study, we showed that the structures that divide the Ucayali and

Marañon basins are bounded by high angle thick-skinned reverse faults so we believe that the degree of deformation above the Peruvian flat slab segment was not properly documented before in the literature.

Flat slab subduction along this part of the South American plate is related to the subduction of the Nazca ridge, which began around 16 Ma. Figures 16 and 17 show Rosenbaum's (2005) reconstruction of the location of the Nazca ridge at 16 Ma, 10 Ma and present day. The shape of the subducted Nazca ridge is deduced from the shape of the Tuamotu Plateau, which is believed to be its conjugate feature on the Pacific plate. One ambiguous point in this reconstruction is whether the northeasternmost tip of the subducted Nazca ridge is present or not (striped area in figure 16). Hampel (2002) argues that it doesn't exist because he postulates that the counterpart mirror image of this tip on the Tuamotu Plateau is a younger feature that was not formed at the spreading ridge. We favor the existence of this portion of the Nazca ridge and following Rosenbaum reconstruction (fig. 16) we observed that from 10 to 4 Ma the subducted Nazca ridge was located beneath the Peruvian fold and thrust belt and the area where the structures mapped in this study (the Contamana high, Contaya high and Moa divisor) are located.

The location of these structures in the Amazonian plain, East from the last thrust in the Andean fold and thrust belt (zone number 4 in figures 16 and 17) is explained as an effect of the propagation of the deformation originated by the higher interplate coupling between a buoyant, thickened Nazca plate and the overriding South America plate. This



deformation would propagate even further to the East as evidence by the existence of a N-S reverse faults system in the Acre basin (Latrubesse and Rancy, 2000).

Based on the seismic interpretation results and the timing described in Rosenbaum's Nazca plate subduction history, we propose that the uplift of the Moa Divisor and the Contamana high as NW-SE oriented structures bounded by high-angle, thick-skinned reverse faults and the reactivation of the Contaya high during the Miocene is related to the subduction of the Nazca ridge from 10 Ma to present. Although precise timing of compression within this band of structural highs is unknown, we suggest that their formation and overall progression began with the Contamana high, and propagated towards the southeast, following the Nazca ridge subduction

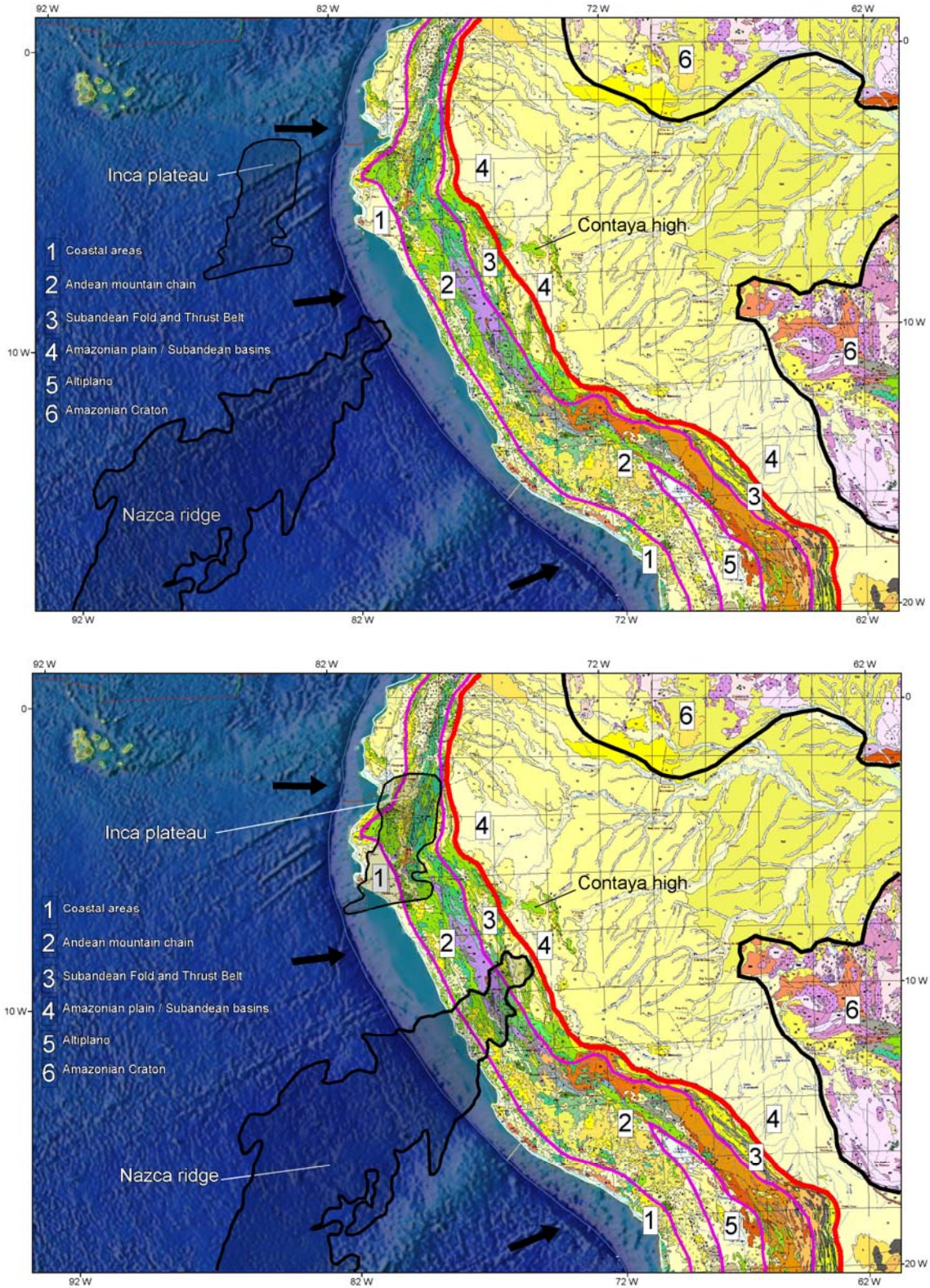


Figure 16. Reconstruction of the subduction history of the Nazca ridge and Inca plateau at 16 Ma and 10 Ma (based on Rosenbaum et al. 2005 reconstruction). The red line represents the limit between the Andean fold and thrust belt and the Amazonia plain.

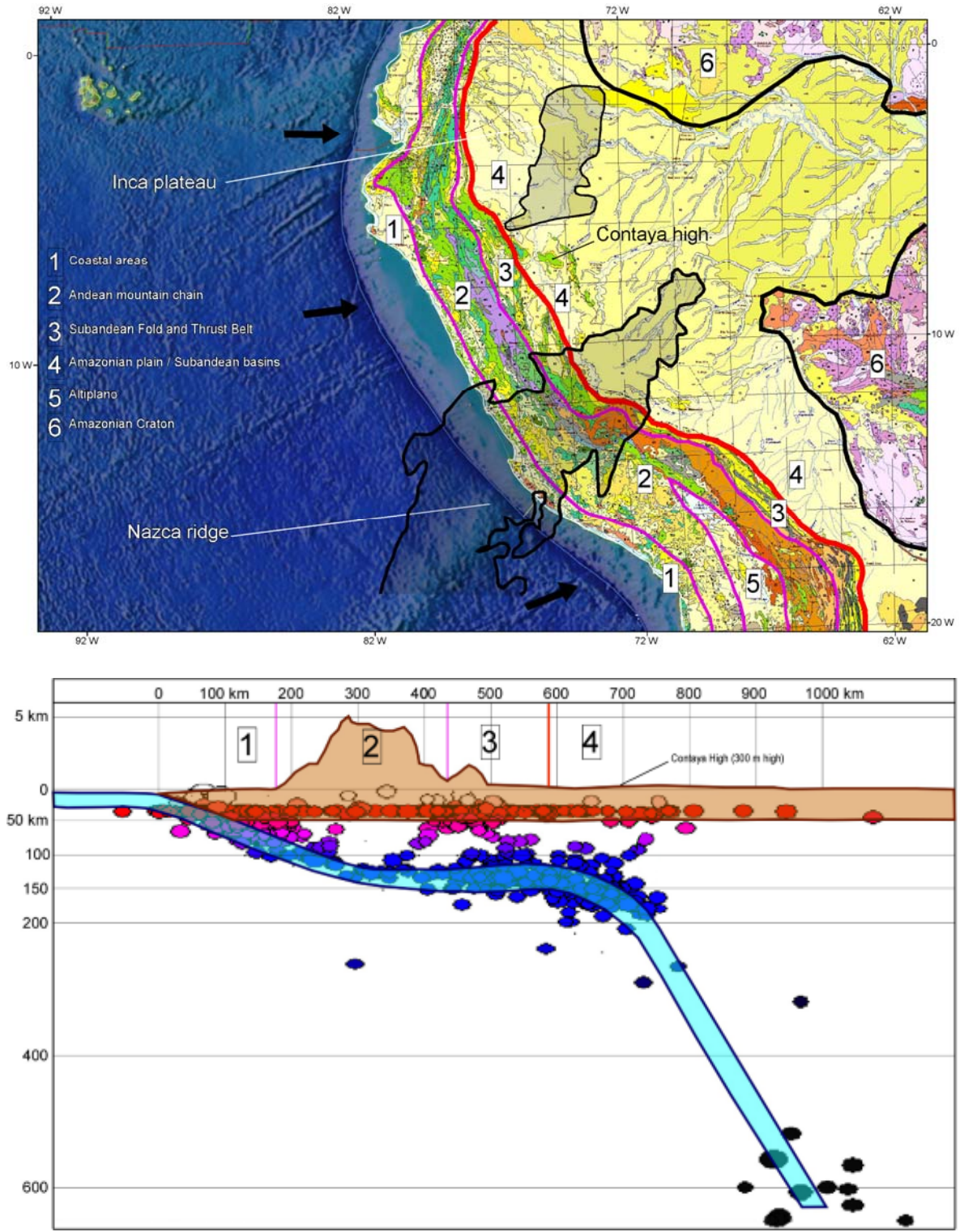


Figure 17. Present day location of the Nazca ridge and Inca plateau and seismological cross section. The seismological cross section shows that the structures that compose the Contaya arch are located above the Peruvian flat slab segment between 5 and 9 South.

## **CHAPTER V**

### **CONCLUSIONS**

The uplifted structures that divide the Marañon and Ucayali basins and compose the Contaya arch are: 1) Tertiary structures that are NW-SE elongated features bounded by thick-skinned high angle reverse faults as seen in the Contamana high and Moa Divisor. 2) Triassic-Jurassic structures as seen in the Contaya high.

Evidence of Devonian to Permian deformation is observed in the seismic sections but their effect on the location of the Tertiary structures is still not well understood. As is the case for the Moa divisor and in other parts of the Ucayali basin, a set of pre-existing Permian-Triassic extensional half grabens were reactivated into reverse faults during the Tertiary. Deformation in the Triassic-Jurassic produced the uplift of the Contaya high and positive structures in the western Ucayali basin that limited the deposition of Pucara Formation and associated salt deposits to the Huallaga and Marañon basins. The uplift of the Moa Divisor and the Contamana high as NW-SE oriented structures bounded by high-angle, thick-skinned reverse faults and the reactivation of the Contaya high during the Miocene is related to the subduction of the Nazca ridge from 10 Ma to present. The location of these structures in the Amazonian plain is explained as an effect of the propagation of the deformation originated by the higher interplate coupling between a buoyant, thickened Nazca plate and the overriding South America plate.

## REFERENCES

- Aceñolaza, F., 2002. Proterozoic-Early Paleozoic evolution in western South America – a discussion. *Tectonophysics* 254, 121-137.
- Alvarez-Calderon, E., 2004. Observed variability in the hydrocarbon systems of the peruvian sub-andean basins, XII Congreso Peruano de Geologia 2004.
- Baby, P., Rivadeneira M., Christophoul F., Barragan R. 1999. Style and timing of deformation in the Oriente basin of Ecuador. Fourth International Symposium on Andean Geodynamics, Göttingen, Germany, 68-72.
- Blakey, R., 2008. Paleogeographic globes. <http://jan.ucc.nau.edu/~rcb7>.
- Bump, A., Kennan, L., Fallon, J., 2008. Deformation history of the Andean foreland, Peru, and its impact on present-day structure. INGEPET 2008 EXPR-3-AB-05
- Cabrera La Rosa, A., Petersen, G., 1936. Reconocimiento geologico de los yacimientos petroliferos del Departamento de Puno, Bol. Cuerpo Ing. Minas Peru 115, 1 – 110.
- Dalmayrac, B., Laubacher, G., Marocco, R. 1988. Caracteres generales de la evolucion geologica de los Andes peruanos. Instituto Geologico Minero y Metalurgico.
- Dunbar, C. O., Newell N. D., 1946. Marine early Permian of the Central Andes and its fusuline faunas, *American Journal of Science* 244, 377 – 402, 457 – 491.
- Espurt, N., Brusset, S., Baby, P., Hermoza, W., Bolaños, R., Uyen, D., Déramond, J., 2008. Paleozoic structural controls on shortening transfer in the Subandean foreland thrust system, Ene and southern Ucayali basins, Peru. *Tectonics* 27, TC3009, doi:10.1029/2007TC002238.
- Fernández, J., Martinez, E., Calderon, Y., Galdos, C., 2002. The Pucara Petroleum System an the pre-Cretaceous sabkha regional seal, a new hydrocarbon play in the Peruvian fold thrust belt: Ingepet 2002 EXPR-3-JF-01.
- Gil, W., 2001. Evolucion lateral de la deformacion de un frenete orogenico. Ph.D. Thesis Universidad Paul Sabatier Toulouse III, 157 pp.
- Gohrbandt, K.H.A., 1992. Paleozoic paleogeographic and depositional developments on the central proto-Pacific margin of Gondwana: Their importance to hydrocarbon accumulation. *Journal of South American Earth Sciences* 6 (4), 267-287.

Gutscher, M.-A., Olivet, J.L., Aslanian, D., Eissen, J.P., Maury, R., 1999. The “lost Inca Plateau”: Cause of flat subduction beneath Peru? *Earth and Planetary Science Letters* 171, 335–341.

Gutscher M.-A., Sparkman, W., Bijwaard, H., Engdahl, R., 2000. Geodynamics of flat subduction: Seismicity and tomographic constraints from the Andean margin. *Tectonics* 19 (5), 814-833.

Gutscher M.-A., 2002. Andean subduction styles and their effect on thermal structure and interpolate coupling. *Journal of South American Earth Sciences* 15, 3-10.

Hampel A. 2002. The migration history of the Nazca ridge along the Peruvian active margin: a re-evaluation. *Earth and Planetary Science letters* 203, 665-679.

Hermoza, W., 2004. Dynamique tectono-sédimentaire et restauration séquentielle du retro-bassin d'avant-pays des Andes centrales. Thèse de l'Université Paul Sabatier de Toulouse III, 296 pp.

Hermoza, W., Brusset, S., Baby, P., Gil, W., Roddaz, M., 2005. The Huallaga foreland basin evolution: Thrust propagation in a deltaic environment, northern Peruvian Andes. *Journal of South American Earth Sciences* 19, 21-34.

INGEMMET Instituto Geologico Minero y Metalurgico del Peru. Serie A: Carta Geologica Nacional. Esc. 1:100000.

Jacques, J., 2004. The influence of intraplate structural accommodation zones on delineating petroleum provinces of the Sub-Andean foreland basins. *Petroleum Geoscience* 10, 1-19.

Jaillard, E., Soler, P., Carlier, G., Mourier, T., 1990. Geodynamic evolution of Northern and Central Andes during early to middle Mesozoic times: A tethyan model. *Journal of the Geological Society of London* 147, 1009-1022.

Jaillard, E., Soler, P., 1996. Cretaceous to early Paleogene tectonic evolution of the northern Central Andes (0-18 degrees S) and its relation to geodynamics. *Tectonophysics* 259, 41-53.

Jaillard, E., Herail, G., Monfret, T., Diaz-Martinez, E., Baby, P., Lavenu, A., Dumont, J.F., 2002a. Tectonic evolution of the Andes of Ecuador, peru, Bolivia, and northernmost Chile. In: Cordani, U., Milani, E., Thomas Filho, A., Campos, D. (Eds.) *Tectonic evolution of South America*, pp. 481-559.

Jaillard, E., Herali, G., Monfret, T., Worner, G., 2002b. Andean geodynamics: Main issues and contributions from the 4th ISAG, Gottingen. *Tectonophysics* 345, 1-15.

Jordan, T., Isacks, B., Allmendinger R.W., Brewer J.A., Ramos V.A., Ando C.J., 1983. Andean tectonics related to the geometry of subducted Nazca plate. *Geological Society of America Bulletin* 94, 341-361.

Kummel, B., 1948. Geological reconnaissance of the Contamana region, Peru. *Geological Society of America Bulletin* 59, 1217 – 1266.

Latrubesse, E., Rancy, A., 2000. Neotectonic influence on tropical rivers of southwestern Amazon during the late Quaternary: The Moa and IPIXUNA river basins, Brazil. *Quaternary International* 72, 67-72

Mathalone, J. M. P., Montoya, R. M., 1995. Petroleum geology of the sub-Andean basins of Peru, In: Tankard, A. J., Suárez, R., and Welsink, H. J. (Eds.) *Petroleum basins of South America: AAPG Memoir vol. 62*, pp. 423–444.

Megard, F., 1979. Estudio geológico de los Andes del Peru central. *Boletín del Instituto Geológico, Minero y Metalúrgico* 8, 207 – 227.

Megard, F., 1984. The Andean orogenic period and its major structures in Central and Northern Peru. *J. Geological Society of London* 141, 893-900.

Navarro, L., Baby, P., Bolaños, R., 2005. Structural style and hydrocarbon potential of the Santiago basin. *INGEPET 2005 EXPR-3-LN-09*.

Newell, N. D., Chronic, J., Robert, T., 1953. Upper Paleozoic of Peru, *Geological Society of America Memoir* 58, 256 pp.

Rosas, S., Fontbote, L., Tankard, A., 2007, Tectonic evolution and paleogeography of the Mesozoic Pucara Basin, central Peru. *Journal of South American Earth Sciences* 24, 1-24.

Rosenbaum, G., Giles, D., Saxon, M., Betts, P., Weinberg, R., Duboz, C., 2005. Subduction of the Nazca ridge and the Inca plateau: Insights into the formation of ore deposits in Peru. *Earth and Planetary Science letters* 239, 18-32.

Seminario, F., Guizado, J., 1976. Síntesis Bioestratigráfica de la Región de la Selva Del Peru, II Congreso Latino Americano de Geología, Caracas, Venezuela, 881–898.

Sempere, T., Carlier, G., Soler, P., Fornari, M., Carlotto, V., Jacay, J., Arispe, O., Neraudeau, D., Cardenas, J., Rosas, S., Jimenez, N., 2002. Late Permian – Middle

Jurassic lithosphere thinning in Peru and Bolivia and its bearing on Andean-age tectonics. *Tectonophysics* 345, 153-181.

Smalley, R., Pujol, J., Reignier, M., Chiu, J-M., Chatelain, J.-L., Isacks, B.L., Araujo, M., Puebla, N., 1993. Basement seismicity beneath the Andean Precordillera thin skinned thrust belt and implications for crustal and lithospheric behavior. *Tectonics* 12, 63-76.

Szekely, T. S., Grose, L. T., 1972. Stratigraphy of the carbonate, black shale and phosphate of the Pucara Group (Upper Triassic-Lower Jurassic), Central Andes, Peru, *Geological Society of America Bulletin* 83, 407 – 428.

Thomas, W., Astini, R., Bayona, G., 2002. Ordovician collision of the Argentine Precordillera with Gondwana, independent of Laurentian Taconic orogeny. *Tectonophysics* 345, 131-152.

Tschopp, H. J., 1953. Oil exploration in the Oriente of Ecuador. *American Association of Petroleum Geologist Bulletin* 37, 2303-2347.

Williams, K. E., 1995, Tectonic subsidence analysis and Paleozoic paleogeography of Gondwana, In: Tankard, A. J., Suárez, R., and Welsink, H. J. (Eds.) *Petroleum basins of South America: AAPG Memoir vol. 62*, pp. 79–100.

Williams, K., 1997. Early Paleozoic Paleogeography of Laurentia and western Gondwana, evidence from tectonic subsidence analysis. *Geology* 25 (8), 747-750

Wine, G., Arcuri, J., Fernández, J., Martinez, E., Calderon, Y., Galdos, C., 2001, Hydrocarbon potential of the Santiago Basin, Peru. PARSEP interim report. 104 pp.

Wine, G., Arcuri, J., Fernández, J., Martinez, E., Calderon, Y., Galdos, C. 2002. Marañon basin technical report. PARSEP interim report. 123 pp.

Wine, G., Arcuri, J., Fernández, J., Martinez, E., Calderon, Y., Galdos, C. 2003. Ucayali/Ene basin technical report. PARSEP interim report. 96 pp.



## VITA

### CONTACT INFORMATION

Luis D. Navarro Zelasco  
luis\_navarro@oxy.com  
1-979-739-3378  
901 Mohawk #79 Bakersfield, CA 93309

### EDUCATION

- Bachelor of Science in Geology. Universidad Nacional San Agustín Arequipa, Peru. March 1998 - December 2002

### PROFESSIONAL EXPERIENCE

- Geologist - Exploration  
Occidental Petroleum Corporation  
Bakersfield, California. May 2008 - present
- Petroleum Geology Lab Instructor  
Texas A&M University  
College Station, Texas. September 2006 - April 2008
- Summer Intern Geologist – Production geology  
Occidental Petroleum Corporation  
Houston, Texas. May - August 2006 and May - August 2007
- Researcher – Petroleum System Analysis  
IRD (Institut de Recherche pour le Developpement)  
Lima, Peru. June 2004 - June 2005
- E&P Data Manager Assistant  
Perupetro  
Lima, Peru. September 2003 - March 2004
- Well Site Geologist Assistant  
Petrobras Peru  
Talara, Peru. January 2003 - July 2003